The Sodium/Iodide Symporter (NIS): Molecular Physiology and Preclinical and Clinical Applications

Silvia Ravera[1,*], **Andrea Reyna-Neyra**[1,*], **Giuseppe Ferrandino**[1,*], **L. Mario Amzel**[2], and **Nancy Carrasco**[1]

[1]Department of Cellular and Molecular Physiology, Yale School of Medicine, New Haven, Connecticut 06510

[2]Department of Biophysics and Biophysical Chemistry, Johns Hopkins University School of Medicine, Baltimore, Maryland 21205

Abstract

Active iodide (I^-) transport in both the thyroid and some extrathyroidal tissues is mediated by the Na^+/I^- symporter (NIS). In the thyroid, NIS-mediated I^- uptake plays a pivotal role in thyroid hormone (TH) biosynthesis. THs are key during embryonic and postembryonic development and critical for cell metabolism at all stages of life. The molecular characterization of NIS in 1996 and the use of radioactive I^- isotopes have led to significan advances in the diagnosis and treatment of thyroid cancer and provide the molecular basis for studies aimed at extending the use of radioiodide treatment in extrathyroidal malignancies. This review focuses on the most recent finding on I^- homeostasis and I^- transport deficiency-causin NIS mutations, as well as current knowledge of the structure/function properties of NIS and NIS regulatory mechanisms. We also discuss employing NIS as a reporter gene using viral vectors and stem cells in imaging, diagnostic, and therapeutic procedures.

Keywords

INTRODUCTION

The thyroid hormones (THs) T_3 (3,5,3′-tri-iodo-L-thyronine) and T_4 (3,5,3′,5′-tetra-iodo-L-thyronine or thyroxine) are crucial for pre- and postnatal development and for intermediary metabolism in virtually all tissues throughout life. Iodide (I^-), an essential constituent of the THs, is actively transported into the thyroid via the Na^+/I^- symporter (NIS), a key plasma membrane glycoprotein. The ability of the thyroid to accumulate I^- was first described by

---

Baumann in 1896 (1, 2). Several decades later, in 1939, radioiodide ($^{131}I^-$) was first used to treat hyperthyroidism (3), and in 1946 it was administered after thyroidectomy to treat thyroid cancer (4). This strategy has become the most effective targeted internal radiation cancer treatment available with far fewer side effects than other treatments (4). The cDNA encoding NIS was isolated in 1996 (5), marking a major breakthrough in thyroid research that led to the subsequent characterization of NIS at the molecular level (6). Functional NIS is found in several extrathyroidal tissues, such as the salivary glands, stomach, and lactating breast, as well as in primary and metastatic breast cancers (7, 8). The latter findings have raised the possibility that NIS-mediated $^{131}I^-$ treatment may be effective in breast cancer.

One of the most remarkable properties of NIS is that it transports different substrates with different stoichiometries. NIS transports I^-, thiocynate (SCN^-) and chlorate (ClO_3^-) with a 2 Na^+:1 anion electrogenic stoichiometry. In contrast, NIS transports perrhenate (ReO_4^-) and perchlorate (ClO_4^-) with a 1 Na^+:1 anion electroneutral stochiometry (9). The anion ClO_4^-, an environmental pollutant previously known only as a competitive inhibitor of NIS, is actively transported by NIS as a substrate (10). Furthermore, NIS is increasingly used as a highly effective reporter gene for imaging techniques (11, 12).

THE IMPORTANCE OF ADEQUATE IODIDE INTAKE AND THYROID HORMONE BIOSYNTHESIS

I^- is a micronutrient essential for human health because it plays a crucial role in TH biosynthesis. In humans, an adequate supply of I^- at the very beginning of life is critical for preventing I^- deficiency disorders (IDDs) that can lead to severe and irreversible cognitive and physical impairments (13, 14). THs are required for the development and maturation of the central nervous system, lungs, and skeletal muscle (15) and are also key regulators of metabolism in all cells (16). Women of reproductive age are one of the demographic groups most susceptible to IDDs because I^- deficiency is directly related to reproductive failure and is associated with perinatal mortality (17, 18). During pregnancy and lactation, a woman's I^- requirement increases from 150 to 250 µg/day. An adequate I^- supply is further essential for nursing mothers because maternal milk is the only source of I^- for newborns. However, the rest of the population can also be affected by I^- deficiency, which may result in low TH production and goiter (enlargement of the thyroid gland) (19). Because of the importance of dietary I^- intake by humans, international organizations, such as the World Health Organization and others, have made an enormous effort to establish guidelines and policies to promote the consumption of salt supplemented with I^- as a strategy for preventing and eradicating IDDs worldwide (20, 21). The oxidized form of I^- (i.e., iodine) is covalently incorporated, a process known as iodine organification, into the protein thyroglobulin (TG), a highly glycosylated homodimer synthesized in the endoplasmic reticulum and stored in the colloid of the thyroid. TG is the precursor of the THs T_3 and T_4, which have 3 and 4 iodine atoms, respectively. THs are released from the colloid into the bloodstream in response to stimulation by thyroid-stimulating hormone (TSH) (for a recent review, see 14) (Figure 1).

MOLECULAR CHARACTERIZATION OF NIS, A UNIQUE MOLECULE IN VERTEBRATES

The use of NIS n-transported I⁻ radioisotopes to diagnose, treat, and monitor thyroid pathologies—a process that takes advantage of the thyroid's ability to accumulate I⁻ via NIS at concentrations up to 40 times those in the plasma under physiological conditions—constitutes a significant advance in clinical practice (3, 22). Fifty years after these strategies were pioneered, Dai et al. (5) isolated the cDNA that encodes NIS by functional screening in *Xenopus laevis* oocytes of a cDNA library prepared from the highly functional rat thyroid-derived FRTL-5 cell line. The isolation of the NIS cDNA has led to a much better understanding at the molecular level of the I⁻ transport process, both in the thyroid and in other tissues, with far-reaching implications both for basic science and for the clinical realm, as described in this review.

NIS is a member of solute carrier family 5A and has been assigned the designation SLC5A5 by the Gene Nomenclature Committee, according to the Human Genome Organization. In rats, NIS is a 618 amino acid protein (5), whereas in humans, it is slightly larger, with 643 amino acids (23, 24). The experimentally tested secondary structure model for NIS shows a hydrophobic protein with 13 transmembrane segments (TMSs), an extracellular amino terminus, and an intracellular carboxy terminus (25, 26). A NIS homology model has been generated (10) based on the only crystal structure available to date for a member of the SLC5A family—the *Vibrio parahaemolyticus* Na⁺/galactose transporter (vSGLT), a bacterial homologue of the human Na⁺/glucose transporter SGLT1 (SLC5A1) (27) (Figure 1). Between core residues 50 and 456, NIS and vSGLT share 32% sequence identity and 64% similarity.

This homology model is key to elucidating the mechanistic requirements of NIS at certain positions and to identifying critical amino acids that significantly affect transport by NIS (see the section titled Iodide Transport Defect-Causing NIS Mutations: From Patient to Molecular Mechanism). Although NIS is *N*-glycosylated at three positions, Levy et al. (28) have shown that *N*-glycosylation is not essential for I⁻ transport or for trafficking NIS to the plasma membrane (29).

NIS-mediated transport of I⁻ into the thyroid is electrogenic and uses as its driving force the Na⁺ gradient generated by the Na⁺/K⁺ ATPase and the electrical potential across the plasma membrane to actively transport 1 I⁻ for every 2 Na⁺. However, NIS transports different substrates with different stoichiometries (Table 1). For example, the stoichiometry of Na⁺/ReO$_4^-$ or ClO$_4^-$ transport is electroneutral (1:1) (9). How NIS binds and releases its substrates remains a key mechanistic question. Recently, Nicola et al. (30) used statistical thermodynamics to show that NIS has a very low intrinsic affinity for I⁻ (K_d = 224 μM), which increases by a factor of 10 (K_d = 22.4 μM) when the transporter has two Na⁺ ions bound to it. This finding sheds light on the long-standing question in the field of how NIS can transport I⁻ so efficiently when the serum I⁻ concentrations are submicromolar and the K_M of NIS for I⁻ is 10–30 μM. Because of the aforementioned increase in affinity, approximately 79% of the NIS molecules are occupied by two Na⁺ ions, enabling them to bind and transport I⁻ highly efficiently at physiological Na⁺ concentrations.

REGULATION OF THYROID NIS

TSH is the primary regulator of NIS in the thyroid at both the transcriptional and post-transcriptional levels (25, 31–35) (see 36 for a recent review). Another regulator of NIS function is I⁻ itself. Wolff & Chaikoff (37) showed that when I⁻ reaches a critical high concentration in the plasma, TH biosynthesis decreases (a.k.a. the Wolff-Chaikoff effect). However, there is an "escape" from this acute Wolff-Chaikoff effect that restores normal TH biosynthesis even in the continued presence of high plasma I⁻ concentrations (38) (see 14 for a recent review). At the molecular level, excess I⁻ may have a deleterious effect on the thyroid by modifying NIS mRNA stability and increasing the production of reactive oxygen species (39, 40).

Among the other mechanisms that regulate NIS is TG (see 41 for extensive discussion). Another level of regulation involves protein–protein interactions that cause plasma membrane proteins to be trafficked to and from the cell surface. One protein that may interact with NIS is the pituitary tumor–transforming gene (PTTG) binding factor (PBF) (42). PBF promotes the intracellular localization of NIS, thereby decreasing I⁻ uptake. PBF has also been associated with thyroid tumorigenesis in vivo (43) and to transformation in vitro. Interestingly, the guanine nucleotide exchange factor for the RhoA GTPase involved in cell adhesion interacts with NIS, activating RhoA and thereby promoting cell invasion and migration of cells expressing NIS (44).

Roepke et al. (45) have reported another level of NIS regulation: The KCNQ1–KCNE2 K^+ channel, which repolarizes cardiac ventricles, forms a constitutively active K^+ channel in thyroid cells. In the thyroid, this channel is stimulated by TSH and is necessary for adequate TH biosynthesis. The same authors showed that KCNE2-null mice developed hypothyroidism owing to decreased I⁻ accumulation in their thyroid. The decrease in I⁻ accumulation was due to impaired NIS-mediated I⁻ uptake, rather than faulty I⁻ organification (46). These findings have led to the discovery that thyroidal NIS function is also regulated by direct cross talk between NIS and a K^+ channel. Interestingly, this was the first interaction reported between a channel and a transporter, and it was followed by the discovery of another physiologically relevant interaction between KCNQ1 and KCNE2 and the Na^+-coupled myoinositol transporter, a member of the same family as NIS found in the choroid plexus of mice (47). These studies make it clear that channels and transporters do not necessarily function in isolation but, instead, they often regulate each other (48).

EXTRATHYROIDAL TISSUE-SPECIFIC ROLES OF FUNCTIONAL NIS AND THEIR PATHOPHYSIOLOGICAL IMPLICATIONS

NIS function is traditionally associated with the thyroid. However, active I⁻ transport has also been also demonstrated in other organs (Figures 2 and 3), including the lacrimal sac and nasolacrimal duct, salivary glands, choroid plexus, stomach, intestine, and lactating breast (14). Reverse transcription polymerase chain reaction (RT-PCR) and immunodetection have further uncovered NIS expression in the kidney, placenta, and ovary (49–53). Recently, Marti-Climent et al. (54) showed the total body distribution of NIS in nonhuman primates by [¹⁸F]-tetrafluoroborate positron emission tomography (PET) (Figure 3).

In the placenta, NIS is expressed at the apical membrane of cytotrophoblasts, where it regulates the transport of I^- from the maternal to the fetal circulation, a process critical for normal fetal thyroid function (49, 55). In the salivary glands, NIS is expressed at the basolateral plasma membrane of epithelial ductal cells, which concentrate I^- (8, 56–58). The secretion of I^- into the saliva is used to diagnose I^- transport defects in newborns by measuring the saliva-to-plasma ratio (normal 20) (14). In the stomach, NIS is expressed at the basolateral surface of the gastric mucosal cells, which release I^- into the gastric juice (56). In the salivary glands and stomach, I^- secretion is considered to serve a protective and healing antimicrobial function (59–62). Interestingly, Altorjay et al. (56) have shown that NIS expression is downregulated in gastric cancer and in intestinal metaplasia, a finding that has led to the suggestion that NIS could be used as a marker in determining the prognosis of patients with stomach malignancies. Because I^- is scarce in the environment, all organisms must use this element optimally to maintain homeostasis, and NIS-mediated secretion of I^- into the lumen of the stomach may help recycle some I^- by allowing it to be reabsorbed in the intestine. Nicola et al. (63) showed that intestinal NIS is expressed at the apical membrane of the enterocytes throughout the small intestine and exhibits similar functional properties to those reported for thyroidal NIS ($K_M = 10$–30 μM). I^- transport by these enterocytes is Na^+-dependent and inhibited by ClO_4^-, suggesting that intestinal NIS is the main conduit by which dietary I^- is absorbed (see 64 for a recent review).

An easy estimate of I^- intake can be made by measuring urinary I^- (65). Spitzweg et al. (53) showed intracellular NIS expression all along the tubular nephron but not at the plasma membrane of these cells. In contrast, using tissue microarray cores from normal human kidney, Wapnir et al. (8) showed staining at the apical surface of the principal and intercalated cells of the renal distal and collecting tubules, suggesting a potential role for NIS in regulating I^- reabsorption. Proteins expressed in the kidney, such as chloride channel 5 (ClC-5) and the Cl^-/HCO_3^- exchanger pendrin, may be involved in I^- metabolism (66, 67). However, although ClC-5 knockout mice developed goiter, their renal I^- transport apparently was not significantly different from that of wild-type (WT) mice (67). Pendrin-null mice have a lower serum I^- concentration than WT mice when challenged with high water intake (approximately twice the usual daily intake) but do not display hypothyroidism. Moreover, limiting the I^- intake of pendrin-null mice did not impair their thyroid function (68, 69). In view of all these reports, generating a kidney-specific NIS-knockout mouse model will be extremely useful in determining the specific role of NIS in renal I^- transport.

As mentioned above, NIS is expressed in the normal breast only late in pregnancy and during lactation (7, 70). Lactation is critical in mammals because maternal milk is the only source of I^- for the newborn. When nonlactating mouse dams are treated with oxytocin alone, their mammary tissue accumulates significantly more radioiodide because it expresses NIS. In contrast, ovariectomized mice require oxytocin, estradiol, and prolactin to express NIS in their mammary glands (7). NIS is also expressed in mammary gland tumors in animal models of breast cancer and, more importantly, in human breast cancer samples. As many as 87% of the breast tumor samples analyzed by Tazebay et al. (7) tested positive for NIS expression, in contrast with 0% of samples of normal nonlactating breast tissue (7, 8). Imaging studies using different substrates of NIS confirm that some breast tumors and their metastases are able to take up radioisotopes, suggesting that it may be possible to diagnose

and even treat these malignancies with radioiodide (71, 72). The disparity between the large percentage of breast tumors that express NIS and the small percentage that display radioiodide uptake may reflect the fact that NIS is not always localized at the plasma membrane. More extensive studies in humans are needed to determine whether metastatic breast cancer can be successfully treated with radioiodide.

In vitro experiments using human breast cancer–derived MCF-7 cells showed that all-*trans*-retinoic acid (atRA) alone (73) or in combination with either dexamethasone (74–76), hydrocor-tisone, or adenosine triphosphate (ATP) induced (77) NIS functional expression. Moreover, in vivo experiments in mice harboring MCF-7 xenografts or in the transgenic breast cancer mouse model [murine mammary tumor virus-polyoma virus middle T antigen (MMTV-PyVT)] showed that atRA induced a significant increase in NIS-mediated radioiodide accumulation compared to what was observed in control mice (78).

It is medically significant that NIS expression is regulated differently in different tissues— by oxytocin, prolactin, and estrogen in the mammary glands, and by TSH in the thyroid. When treating extrathyroidal cancers, it is possible to protect the thyroid from radiation by administering THs to lower TSH levels (72). This strategy can be used both when treating cancers that express NIS endogenously (e.g., breast cancer) and when treating cancers that have been made to express NIS exogenously by gene transfer (see below).

As for the female reproductive organs, $^{125}I^-$ autoradiography of the oviduct and luminal epithelium of the uterus in rats shows that these two tissues concentrate I^-, as reported by Brown-Grant (79). Since then, other studies have investigated NIS expression in the normal or cancerous female reproductive tract. Using human tissue microarrays and affinity-purified antihuman NIS antibodies, Wapnir et al. (8) determined that 56% of 25 endometrial carcinomas examined showed weak NIS immunoreactivity. NIS staining has been reported in human placental endometrial glands during the first trimester of pregnancy (49). NIS expression was also observed in endometrial biopsies from postmenopausal (57%) and sterile (60%) women and to a lesser extent (20%) in samples from fertile women (80). These results suggest that NIS may be usable as a biomarker for distinguishing between sterile and fertile endometrial mucosa, which is currently not possible with conventional staining (80). Further studies using more human tissue samples will be necessary to determine whether NIS can indeed serve as a fertility marker.

Although several groups have reported that NIS is expressed in the human ovary (52, 81, 82), Riesco-Eizaguirre and colleagues (52) showed by functional assays and immunoblot experiments that NIS is expressed not only in the ovary but also in the fallopian tube in humans and female rats. These authors showed that the electrophoretic mobility of ovarian NIS is similar to that of rat thyroid NIS. Moreover, during the estrous cycle in rats injected with $^{125}I^-$, uptake of I^- increases significantly in early proestrus, which coincides with a significant rise in estradiol levels and follicular maturation (83). They also performed whole-body scans on 345 female patients diagnosed with thyroid pathologies but no ovarian dysfunction, using the NIS substrate $^{99m}TcO_4^-$ as a tracer. Of these patients, 15% showed $^{99m}TcO_4^-$ accumulation in the ovarian/fallopian tube region. These results suggest that radioiodide treatment for women with thyroid malignancies should be scheduled for the

nonovulatory period of their menstrual cycle to decrease the probability that the radioiodide could damage their ovaries. Furthermore, this study supports the notion that radioiodide could potentially be used to treat ovarian cancer, one of the most devastating malignancies in women, and one that has a very low (45%) 5-year survival rate after diagnosis. Riesco-Eizaguirre et al. (52) showed that 98.9% of the biopsies from ovarian cancer patients that they analyzed expressed NIS, and one-third of these samples showed expression at the plasma membrane, which would be key for leveraging radioiodide as an effective therapeutic tool. Taken together, these findings suggest that NIS could potentially be used to diagnose and treat ovarian cancer.

IODIDE TRANSPORT DEFECT-CAUSING NIS MUTATIONS: FROM PATIENT TO MOLECULAR MECHANISM

Congenital hypothyroidism (CH) is a condition that occurs in 1 in 2,000–4,000 live births worldwide, which leads to goiter and impaired physical and mental development when not diagnosed immediately after birth and left untreated (84, 85). For this reason, newborns have their thyroids screened in most developed countries. CH can be caused by thyroid dysgenesis induced by mutations in genes such as *NKX2-1*, *PAX8*, and *NKX2-5*, which encode transcription factors essential for thyroid gland development (86–90). CH can also be caused by secondary hypothyroidism when genetic defects impair the function of the hypothalamic/pituitary axis and by dyshormonogenesis when genetic defects impair key components of TH biosynthesis, such as TSH receptor, NIS, TG, thyroid peroxidase, dual oxidase 2, or IYD (iodotyrosine deiodinase) (91–96).

CH-causing mutations in the SLC5A5 gene, which encodes NIS, induce a condition that is known as I^- transport defect (ITD) and results in impaired I^- accumulation in the thyroid. ITD is a rare autosomal recessive condition that is diagnosed by reduced or absent thyroidal I^- uptake and a low saliva-to-plasma I^- ratio (<20). To date, 14 ITD missense and nonsense mutations have been reported that affect the NIS coding sequence: V59E (97), G93R (10), R124H (98), 143-323 (99), Q267E (100), V270E (101), C272X, 287-288 (102), T354P (103, 104), G395R (105), 439-443 (106), G543E (107), fs515X, and Y531X (108). One mutation in the 5′ untranslated region (a C→T transition at position −54) has also been reported (109). In the absence of a crystal structure for NIS, valuable mechanistic and structural information on the protein has been obtained by characterizing the amino acid positions that have been found mutated in patients with ITD.

ITD-causing mutations in NIS span the whole SLC5A5 gene, affecting NIS in a variety of positions from the N-terminus to the C-terminus. These mutations are remarkably useful in revealing regions of the protein that are essential to its function. Significant mechanistic insights have been gained by determining how these human ITD mutations affect NIS folding, plasma membrane targeting, and activity and by interpreting the results of these mutations in the light of the NIS homology model (10, 98, 106). This approach has made it possible to determine the molecular requirements for NIS function that must be met at the aforementioned positions. The mutations that have been studied from a mechanistic standpoint are described below and summarized in Figure 4. Their location within the NIS

molecule and their degree of conservation throughout the SLC5 family are shown in Figures 1, 4, and 5.

NIS MUTANTS THAT ARE EXPRESSED AT THE PLASMA MEMBRANE BUT ARE INTRINSICALLY INACTIVE

The V59E NIS mutation was discovered as a compound heterozygous mutation in all three children of a Japanese couple in 2000. The patients inherited the T354P and V59E NIS mutations from their healthy mother and father, respectively. Reed-Tsur et al. (97) showed that heterologous expression of the single V59E NIS mutant in COS7 cells resulted in a NIS protein that is properly targeted to the plasma membrane but is intrinsically inactive, showing that a charged amino acid at position 59 impairs NIS function. However, the protein remains active if a neutral amino acid other than Pro occupies that position. Their data further suggested that position 59 is involved in intramembrane helix–helix contact, which is consistent with the NIS homology model showing V59 in contact with TMS 8.

The G93R NIS mutation was identified in a Japanese patient who developed goitrous hypothyroidism due to a compound heterozygous G93R/T354P NIS mutation. G93R NIS is properly targeted to the plasma membrane in COS7 cells but lacks activity; this is not due to a positively charged residue within the membrane, as G93K NIS is active. Instead, substitutions at position 93 significantly change the K_M of NIS for I^-. This is true not only of neutral residues (Thr, Asn, and Gln) but also of charged residues (Asp and Glu), indicating that NIS tolerates either a basic residue (e.g., Lys) or an acidic residue (e.g., Asp or Glu) in the middle of TMS 3. As described above, NIS is an electrogenic cotransporter of I^- with a $2Na^+$:$1I^-$ stoichiometry (9) and also an electroneutral cotransporter of ReO_4^- and ClO_4^- with a $1Na^+$:1 anion stoichiometry. Strikingly, replacing G93 with a Thr or an Asn converts NIS-mediated ReO_4^- or ClO_4^- transport from electroneutral to electrogenic. The G93T NIS mutant shows an increased K_M for I^-, ReO_4^-, and Na^+. Moreover, G93E and G93Q NIS transport ReO_4^- and ClO_4^-, even though I^- transport is severely impaired in these two mutants, indicating that Glu and Gln confer on NIS the ability to discriminate between substrates. Paroder-Belenitsky et al. (9) could interpret the biochemical results they obtained by replacing G93 with other residues by using their NIS homology model, in which G93 makes contact with W255, which is located in TMS 7. The G93/W255 pair can be described as a ball-and-socket joint, with the CαH of Gly representing the ball and the six-member ring of Trp representing the socket. Position 93 appears to be a pivot around which occurs a major conformational change between the inwardly and the outwardly open conformation. In the NIS model, when G93 is replaced by another amino acid, the side chains of the nonglycine residues point toward the inside of the cavity occupied by the substrates (Na^+ and anion). The specific properties of the side chain of the residue placed at position 93 affect the way the transporter interacts with its substrates, as demonstrated experimentally.

The T354P NIS mutant was first identified in a Japanese ITD patient bearing a homozygous missense mutation. T354P NIS and other position-354 NIS mutants are properly targeted to the plasma membrane, but most mutants are inactive (104). NIS activity is preserved only

when T354 is replaced with a Ser, indicating that a β–OH group is crucial at this position. Interestingly, mutants that are inactive at physiological concentrations of Na^+ (140 mM) show low but significant levels of activity when the $[Na^+]$ is doubled. TMS 9 of NIS contains the highest number of Ser and Thr residues of any NIS TMS. Replacing those residues with other amino acids produced NIS mutants with a lower apparent affinity for Na^+ than WT NIS. The high-resolution structure of the bacterial leucine transporter (LeuT), a member of the SLC6 family, shows a Na^+ atom (Na1) sharing the same cavity as the substrate leucine, and a second Na^+ atom (Na2) coordinated by residues T354 and S355, which correspond to S353 and T354 of NIS, respectively. On the basis of the crystal structure of LeuT (110) and the molecular characterization of positions 353 and 354 of NIS, De la Vieja et al. (103) predicted that NIS should have the same fold as LeuT, despite the lack of primary sequence homology between the two. They also expected that S353 and T354 of NIS should form the so-called Na2 binding site. This prediction was confirmed when the crystal structure of the bacterial Na^+/galactose transporter vSGLT, a member of the SLC5 family, became available (vSGLT and LeuT share the same fold). The characterization of other Na^+-dependent transporters showed that the architecture of the Na2 binding site is also conserved in other families, such as the betaine/carnitine/choline family (111), and in nucleobase/cation symporter-1 (NCS1) (112). By carrying out scintillation proximity assays, Ravera et al. (113) demonstrated that the double mutant S353A/T354A still binds two Na^+ ions but the cooperativity observed in binding experiments with WT NIS was lost. Furthermore, the pronounced changes in the K_d values for Na^+ in the double mutant ($K_{d,Na1}$ = 0.9 mM and $K_{d,Na2}$ = 80.5 mM; by comparison, the values for WT NIS are $K_{d,Na1}$ = 112.5 mM and $K_{d,Na2}$ = 9.2 mM) strongly suggest that the affinity of the Na1 site is increased in the mutant because it does not have to "pay" for the conformational change that increases the affinity of Na2. Consequently, Na^+ binds to Na1 first. This binding order is the opposite of that proposed for other transporters (114–116).

The *G395R* NIS mutation was first described in several members of a large family with a history of ITD. The patients belong to the Hutterite group of central Canada, whose members live in geographical and cultural isolation and have a high degree of consanguinity. Replacing G395 with other residues does not affect NIS plasma membrane targeting, as Dohán et al. (105) showed by immunofluorescence and cell surface biotinylation. They found that position 395 does not tolerate charged residues. The only NIS mutants that preserve any I^- uptake are *G395A* and *G395S*, which exhibit 70% and 30% the activity of the WT, respectively, indicating that a residue with a small side chain is essential at position 395. G395 is close to residues located in TMS 4 in the NIS homology model.

NIS MUTANTS THAT ARE TARGETED TO THE PLASMA MEMBRANE BUT RETAIN MINIMAL ACTIVITY

Q267E NIS was discovered in an American ITD patient with a compound heterozygous mutation: In the maternal allele, the patient had a cytosine-to-guanidine substitution at nucleotide 1940 in exon 13, generating the NIS mutant *Y531X*. In the paternal allele, the patient had a cytosine-to-guanidine substitution at nucleotide 1146 (exon 6), which resulted in a Glu-to-Gln replacement (Q267E). Biochemical studies show that Q267E NIS is

properly targeted to the plasma membrane but preserves very little activity. Other amino acid substitutions at position 267 indicate that charged side chains are not tolerated at that position; by contrast, replacing Q267 with amino acids bearing a neutral side chain resulted in NIS mutants that were partially active (with 20–30% the activity of WT NIS). The kinetic parameters obtained for the Q267 mutants show that their reduced or absent I⁻ uptake is due to a lowered V_{max}: The apparent affinities of these mutants for I⁻ and Na⁺ are similar to those of WT NIS. Taken together, these observations demonstrate that Q267 mediates important interactions that take place during the conformational changes essential for the transport cycle and that position 267 is not involved in substrate binding (100). The NIS homology model shows that Q267 interacts with TMS 3.

NIS MUTANTS THAT ARE INTRACELLULARLY RETAINED

The ITD-causing mutation *R124H* was identified as a homozygous transition at nucleotide 718 in the second exon of the SLC5A5 gene in a French patient. R124H NIS is intracellularly retained, as shown by flow cytometry analysis and cell surface biotinylation, but it is intrinsically active: Membrane vesicles prepared from COS7 cells expressing R124H NIS show ClO_4^--sensitive I⁻ uptake. Replacing R124 with other charged or certain uncharged amino acids does not recover plasma membrane targeting. R124Q NIS, by contrast, is targeted to the plasma membrane and avidly accumulates I⁻, indicating that a δ-amino group is required at position 124 of NIS. The NIS homology model shows C440 as a residue that may interact with the δ-amino group of R- or Q124. Although C440A NIS is active, the double mutant *C440A-R124Q* NIS is both intracellularly retained and completely inactive, indicating that the interaction between the δ-amino group at position 124 and the thiol at position 440 is essential for correct NIS folding and plasma membrane targeting (117).

Another ITD-causing mutant, *439-443* NIS, was first described in an Italian CH patient with a homozygous mutation. The 439–443 deletion results in a protein which is both inactive and not targeted to the plasma membrane in COS7 cells. Engineering five Ala residues at the positions of the missing amino acids significantly improves cell surface targeting and partially recovers I⁻ transport. Interestingly, engineering an Asn at position 441 within a 4-Ala background completely restores NIS activity, and Gln has the same effect. On the basis of the NIS homology model, Li et al. (106) proposed that N441 participates in the α-helix N-capping that occurs in TMS 12, as follows. Within the 4-Ala background, N441 mediates the N-capping of TMS 12, restoring NIS activity. By contrast, an Asn or Gln at position 440 produces an inactive mutant, possibly because, in the resulting mutants, the distance between N440 or Q440 and TMS 12 is too great for N-capping to occur.

The *G543E* NIS mutation was detected in two Japanese siblings carrying a homozygous mutation. De la Vieja et al. (107) demonstrated that G543E NIS is not targeted to the plasma membrane and is intrinsically inactive, as shown by I⁻ transport in membrane vesicles obtained from cells expressing this mutant protein. G543E NIS matures only partially and is endoglycosidase (endo) H sensitive, indicating that it is retained at some point before the medial-Golgi, the site where endo H resistance is conferred on proteins. Substitutions at

position 543 show that neither negative nor positive charges are tolerated at that position, and the only neutral amino acids that can be engineered there to produce an active protein are Ala and Ser.

NIS MUTANTS THAT ARE DEFECTIVELY TARGETED TO THE PLASMA MEMBRANE BUT FULLY ACTIVE

The *V270E* NIS mutation was found as a compound heterozygous mutation in an American patient (101). The maternal allele encodes the *V270E* NIS mutant, whereas the paternal allele encodes R124H NIS. In COS7 cells, V270E NIS showed very low residual activity due to a defect in plasma membrane targeting: Membrane vesicles expressing V270E NIS avidly accumulated I^-. Interestingly, the patient expressing V270E/R124H NIS developed hypothyroidism in childhood. In contrast, the ITD patient bearing the homozygous *R124H* NIS mutation developed CH with significant clinical manifestations as a newborn. This difference in the age of presentation may be due to residual V270E NIS activity, an explanation compatible with the patient's reduced, although not absent, $^{123}I^-$ uptake, which was revealed by thyroid scintigraphy. The increase in TSH levels following a reduction in TH production might have partially overcome the defect in trafficking of V270E NIS to the plasma membrane by enhancing NIS transcription. The impaired plasma membrane targeting of the *V270E* NIS mutant could be the result of a change in the surface charge of a positive patch in the intracellularly facing domain of the NIS molecule, which may hinder interactions between NIS and proteins key for its trafficking to the cell surface. Consistent with this possibility, increasing the amount of positive charge in the patch by introducing Arg or Lys at position 270 partially restored plasma membrane targeting. Unsurprisingly, when the original Val was replaced with Ile or even Leu, plasma membrane targeting was mostly retained (101).

In summary, the detailed molecular characterization of NIS mutants found in patients and the effects of various amino acid substitutions at the mutated positions have yielded key mechanistic information about the specificity, stoichiometry, coupling, and binding order of the substrates of NIS.

NIS GENE TRANSFER: IMAGING AND RADIOTHERAPY

In the last two decades, NIS has become an important player in the use and optimization of gene therapy owing to its capacity as a reporter and as a therapeutic gene. In 1997, Shimura and colleagues (118) were the first to use NIS in gene transfer therapy. They were able to isolate a clonal variant of the FRTL line, FRTL-Tc, that forms tumors in rat subcutaneous tissue, metastasizes to the lungs and liver, and loses its ability to accumulate I^-. They then transduced FRTL-Tc cells with rat NIS (rNIS) to generate the stable cell line Tc-rNIS, which expresses rNIS and is capable of accumulating I^-. Injecting Tc-rNIS into rat subcutaneous tissue results in tumors that can be imaged by delivering $^{125}I^-$ to them (118). This study was the first to suggest that NIS could be introduced into virtually any cell or tissue for imaging and/or therapeutic purposes.

NIS is becoming the counterpart for human studies of green fluorescent protein and luciferase, which have been used extensively in cells and other organisms. Since Shimura and colleagues' original study (118), NIS has been used as a reporter gene to investigate the pharmacokinetics and pharmacodynamics of several viral agents (11). NIS offers several advantages over other reporter genes, such as herpes virus thymidine kinase, the dopamine-2 receptor, somatostatin receptor 2, and the norepinephrine transporter (11). NIS expression and activity correlate with cell viability because only living cells can accumulate I^-. NIS also offers higher detection sensitivity, because it actively transports its substrates rather than simply binding a substrate stoichiometrically. Moreover, NIS can translocate a variety of substrates, which can be detected using different systems, such as gamma cameras, PET, and SPECT (single-photon emission computed tomography) combined with computed tomography (CT) (Table 1). NIS-based gene transfer methodology can be divided into four categories: (*a*) replication-defective virus–mediated gene therapy, (*b*) replication-competent/ oncolytic virus–mediated gene therapy, (*c*) stem cell biodistribution and survival, and (*d*) regenerative medicine.

REPLICATION-DEFECTIVE VECTORS

In virus-mediated gene therapy, viral vectors that do not lyse cells allow the insertion of therapeutic genes into the cell genome. This is used extensively in cancer therapy. NIS is one gene of choice in this approach, because when NIS is expressed in cells, they translocate radioisotopes that can be used for imaging or therapeutic purposes (119–123), thereby making it possible to determine the appropriate dose of radioisotope to use in therapy (124, 125).

NIS is used as a reporter gene to optimize the vector, dosage, and delivery of a second therapeutic gene. A classic example of this was shown by Niu and coworkers in 2004 (126); the objective of the study was to develop a gene therapy procedure for cystic fibrosis patients by replacing the nonfunctional *CFTR* gene with a functional copy. The use of NIS made it possible to optimize the vector used for the gene transfer of the functional *CFTR*. NIS was delivered to the lung in rats via an adenoviral vector, and its activity was monitored by $^{99}TcO_4^-$ scintigraphy and $^{124}I^-$ PET to follow the distribution, intensity, and duration of the pulmonary gene transfer. After 17 days, NIS was still detectable in the lungs (126).

REPLICATION-COMPETENT ONCOLYTIC VIRUSES

Replication-competent oncolytic viruses (RCOVs) are increasingly used in cancer therapy studies because they can specifically target cancer cells and amplify the expression of vector-associated genes. RCOVs, such as parvoviruses, reoviruses, the mumps virus, and the Moloney murine leukemia virus display a spontaneous tropism for cancer cells. Others, such as the adenovirus, herpes simplex virus, measles virus (MV), vesicular stomatitis virus, and vaccinia virus (VV), have been engineered to specifically target cancer cells. RCOVs usually control the molecular machinery of cell death, inducing apoptosis, but only after exploiting all the resources of the cell to synthesize and assemble new viruses that will infect surrounding cells. The targeting of RCOVs involves the use of specific surface markers expressed by the tumor cells as receptors for virus entry or cofactors for viral gene

expression—e.g., the folate receptor, CD20, the prostate-specific membrane antigen, and the androgen and estrogen receptors. However, oncolytic virus therapy still presents many challenges, including variability in the preclinical and clinical response, the limited efficiency of transducing tumors, and the limited extent of infection within the tumor. The immunogenicity of the viruses needs to be optimized to modulate the organism's immune response to allow the virus to replicate and be distributed.

To address these issues, it is necessary to efficiently monitor the path of the viral particles, the numbers of targeted and infected cells, and the duration and propagation of the viral infection. Functional NIS expression correlates with the duration of viral expression and makes it possible to follow the uptake of the radioisotope throughout the viral infection cycle within the tumor (11). At the onset of infection, the NIS gene is translated and the protein is targeted to the plasma membrane, making it possible to detect the accumulated radiotracer. At the peak of active replication, radiotracer uptake is at its maximum; it will drop during the prelytic phase of the infection. After cell lysis, the assembled viral particles are released, and the infection is propagated, with NIS being expressed in neighboring cells. This strategy is used in different tumor cell lines. Msaouel et al. (127) reported a correlation between NIS expression with I^- accumulation and cell death in nude mice injected with LNCaP cells (a prostate cancer cell line) that were infected with an MV carrying NIS. Peerlinck and colleagues (128) showed a correlation between radiotracer accumulation and cell viability in xenografts generated with colorectal carcinoma cells in nude mice. Using nanoSPECT/CT and immunohistochemistry (IHC), they observed that $^{131}I^-$ accumulated in the first 48 h postinfection. After 48 h, I^- accumulation decreased, NIS was no longer detectable at the plasma membrane, and the cells were dying (128). Haddad and colleagues (129) sequentially imaged a pancreatic tumor infected with a VV encoding NIS. They monitored NIS expression using radiotracer accumulation and IHC in explanted tumors at different stages of infection, observing that cell death was linked to decreased I^- uptake.

NIS-mediated imaging also makes it possible to study the distribution of viral infection throughout the whole body because NIS-mediated I^- uptake is localized to the sites of infection as well as sites of physiological NIS-mediated I^- accumulation, such as the thyroid, stomach, lactating mammary glands, salivary glands, and kidney; the bladder also lights up on the scan, being the site of excretion of the radioisotope. Systemic administration of a tumor-specific virus encoding NIS will also make it possible to image and treat metastatic lesions (130) and to detect positive surgical margins after resection of a tumor (131).

Miller & Russell (11) have shown that the specificity within tumors of systemically administered replicating oncolytic viruses can be effectively monitored using NIS-mediated imaging. Biodistribution imaging can be used to screen tumors susceptible to oncolytic virus therapy and to optimize the vector design for targeted therapies, taking advantage of cancer-selective mucin 1-expressing, carcinoembryonic antigen–expressing, α-fetoprotein-expressing, estrogen-positive, and androgen-positive tumor cells. This type of imaging is significantly improved by using NIS (132–137).

Measles Virus

Edmonston vaccine strains of MV display significant antitumor activity; they bind to the receptor CD46, which is highly expressed in some cancers (138, 139). When engineered to express NIS (MV-NIS), these strains facilitate localization of viral gene expression and offer a tool for tumor radiovirotherapy. MV-NIS was successfully employed as an oncolytic reporter for oncolytic virus therapy by several investigators in preclinical studies on ovarian cancer (140), pancreatic cancer (12), prostate cancer (127), mesothelioma (131), hepatocellular carcinoma (141), osteosarcoma (142), and endometrial cancer (143).

Russell et al. (130) used intravenous infusion of MV-NIS to treat two measles-seronegative patients with relapsing drug-refractory myeloma and multiple glucose-avid plasmacytomas. Remarkably, both patients responded to the therapy, and one went into complete remission (130).

Galanis et al. (140) clinically assessed the effectiveness of MV-NIS in patients with taxol- and platinum-resistant ovarian cancer. MV-NIS was administered intraperitoneally every 4 weeks for up to 6 cycles. After treatment, NIS expression in the tumors was confirmed in three patients (Figure 6) by $^{123}I^-$ uptake visible on SPECT/CT scans and was associated with prolonged progression-free survival. Post-treatment, immune monitoring of patients showed that their T cells recognized tumor antigens better than before the treatment, suggesting that the MV-NIS treatment triggered cellular immunity against the patients' tumors (140). Currently, 10 clinical trials in which MV-NIS is being administered to treat different types of cancer may be found at the website of the US National Institutes of Health (https://clinicaltrials.gov/).

Vaccinia Virus

VV is one of the emergent oncolytic viruses that have been used successfully to treat cancer. Its oncolytic activity has been documented in several in vitro and in vivo studies. VV carrying the human NIS gene has been investigated as a possible treatment for endometrial cancer (144), pancreatic cancer (145, 146), malignant pleural mesothelioma (147), and gastric cancer (148) by in vitro and in vivo monitoring of infection, distribution, and cytotoxicity. Tumor growth and reduction were measured by $^{99m}TcO_4^-$ and $^{124}I^-$ SPECT/CT. In colorectal peritoneal carcinomatosis, the same assessment was carried out by $^{131}I^-$ SPECT/CT (149).

VV carrying NIS was used as an imaging tool to identify positive surgical margins of breast cancer in a murine model (150). Ninety percent of the tumors xenografted into the mammary fat pad were surgically resected and subsequently injected with VV-NIS in the surgical wound. $^{124}I^-$ microPET images showed that fewer than 10% of cells were still alive five days after treatment (150). VV carrying NIS was also successfully used in a combined therapy with radionuclides, exploiting the induced capability of the infected cells to actively accumulate $^{131}I^-$, as reported by Gholami et al. (151) for anaplastic thyroid tumors that had lost their ability to accumulate I^- and by Mansfield et al. (152) for prostate cancer. In vivo experiments in nude mice harboring xenografts derived from human prostate PC3 cells showed that combining virus therapy (VV-NIS) and iodizing radiation did not adversely

affect oncolysis. Moreover, combining radioiodide and infection of tumors with VV-NIS was more effective than either therapy alone (152).

NIS AS A VALUABLE MOLECULE TO MONITOR THE FATE OF STEM CELLS

Stem cells are currently being investigated as a potential therapeutic tool for several disorders in small and large animals. One of the main challenges of this approach is determining the viability of the cells after they are transplanted.

Pluripotent stem cell (PSC)–based therapies have the potential to restore the function of permanently damaged organs because these cells can be differentiated in vitro into any cell type. However, they introduce the risk of forming teratomas. To study this phenomenon, Lehner and colleagues (153) generated murine PSCs stably expressing human NIS (hNIS) and injected them into mice to induce teratoma formation. By $^{124}I^-$ PET, they monitored the growth of the teratomas and reported a correlation between tumor mass and tracer uptake. They observed that hNIS expression and $^{124}I^-$ did not affect the viability or the differentiation of PSCs and concluded that NIS-mediated $^{124}I^-$ uptake can be used to monitor the formation of potential teratomas when PSCs are injected (153).

Stem Cells and Cancer

Another emerging cancer therapy is one based on engineering mesenchymal stem cells (MSCs) to function as vehicles for delivering specific reporter or therapeutic genes to tumors. MSCs spontaneously migrate to damaged tissue and are actively recruited to solid tumors (154). MSCs can be engineered to express NIS to selectively deliver radionuclides for better visualization and effective treatment of metastases. Indeed, NIS has been successfully used to detect and treat colorectal cancer metastases in rat liver in a model involving colorectal carcinoma LS174t cells injected into nude mice. When NIS-expressing MSCs were injected systemically into this model, $^{131}I^-$-treated mice displayed a 40% reduction in liver metastases when compared to control mice (154).

One main goal of modern oncology is to first understand and then find a way to eliminate cancer stem cells (CSCs). CSCs are a unique self-renewing population of cells critical for tumor progression, metastasis formation, and recurrence. An important step in reaching this goal is developing a reliable method for identifying these cells and determining how potential treatments might affect their survival. Using $^{124}I^-$ PET, Park et al. (155) studied the microenvironment conditions that promote early survival of implanted NIS-expressing CSCs. They investigated early engraftment and survival of CSCs in mice and reported that more $^{124}I^-$ is taken up when CSCs are implanted into ischemic limbs than when they are implanted into nonischemic limbs. They concluded that NIS imaging can help determine the conditions that promote early survival of implanted CSCs (155).

Stem Cells in the Central Nervous System

Stem cells are a potential therapeutic tool for several neurological disorders and for traumatic brain and spinal cord injury. Interestingly, after neural stem cells (NSCs) are transplanted into the brain, hNIS can be used as a reporter gene for tracking and visualizing

NSCs in vivo without affecting the ability of NSCs to generate neuronal and glial cells in vitro or in vivo (156).

Stem Cells and Cardiac Repair

Because damaged myocardial cells are not replaced, there is a loss of tissue functionality after a myocardial infarction (MI). An important goal in cardiology is to find a way to replace damaged cells with functional ones to restore the functionality of the heart. Differentiated stem cells are used for this purpose. However, it is critical for optimizing the methodology to develop improved strategies for longitudinally tracking engraftment of these cells. One of the first reports on NIS imaging in cardiac repair was a study by Terrovitis et al. (157), in which rat cardiac-derived stem cells (rCDSCs) were transduced via lentiviral vectors carrying the NIS cDNA. Following coronary artery ligation, the authors injected NIS(+) rCDSCs directly into the myocardium of the rats. NIS expression in rCDSCs did not affect cell viability or proliferation, and it was possible to visualize the cells by $^{124}I^-$ SPECT up to 6 days postinjection (157).

Templin et al. (158) reported for the first time the possibility of monitoring the viability and tissue distribution of cellular grafts in pigs with MI over a long period of time. Transgenic human-induced pluripotent stem cells stably expressing a fluorescent reporter and NIS were assessed in vitro for I^- uptake, efflux, and viability. Ten days after induction of MI, the cells were injected into the myocardium and imaged via dual-isotope SPECT/CT with $^{99m}TcO_4^-$ and $^{123}I^-$. The injected cells could be successfully visualized for up to 15 weeks post-transplantation, and importantly, they did not form any teratomas (158).

Lee and coworkers (159) transfected NIS into canine stem cells using an adenovirus and then injected these cells into beagles intramyocardially. Implantation of the cells and their viability were monitored by $^{99m}TcO_4^-$ SPECT (159). A similar approach was used by Shi and coworkers (160). They engineered bone marrow–derived mesenchymal stem cells (BMSCs) using a lentiviral vector expressing NIS and transplanted them into rat infarcted myocardium. $^{99m}TcO_4^-$ SPECT/CT imaging was done in vivo 1 week post-transplantation, revealing that the BMSCs differentiated into adipocytes and osteoblasts and that NIS expression was stable for up to 3 weeks (160). They also investigated the effect of hypoxia-inducible factor 1α (HIF-1α), which induces transcription of numerous proangiogenic genes, on the survival of the BMSCs. Micro-PET/CT and echocardiography were compared as to their utility in helping evaluate therapeutic effects (161). Rat BMSCs transduced with lentivirus expressing HIF-1α and NIS were transplanted into a rat MI model. The study reports higher expression of vascular endothelial growth factor and angiogenin 4 (Ang-4), improved metabolism, and less fibrotic tissue. Furthermore, the transplanted HIF-1α/NIS-transduced BMSCs mainly differentiated into endothelial cells, creating new blood vessels in the MI zone. Metabolic activity and cardiac function significantly increased at 4 weeks (161).

Chang and colleagues (162) transduced NIS into cardiosphere-derived cells (CDCs) to determine how different methods of cell separation prior to injection would affect cell metabolism and bioenergetics and ultimately the efficiency of the engraftment of the cells.

Their results may eventually help optimize the preparation conditions for CDC transplantation.

The study of cell differentiation is becoming increasingly important. One approach that is currently being pursued in the context of cardiomyocytes is the generation of a transgenic reporter line that expresses NIS under the control of the α-myosin heavy chain promoter. The myocardium of transgenic mice showed rapid and intense uptake of $^{131}I^-$, higher than the thyroid, and was also clearly visualized on $^{124}I^-$ microPET. $^{124}I^-$ uptake in the heart was completely blocked by ClO_4^-. These transgenic mice can be used to study cardiomyocyte-specific reporter gene expression and cellular differentiation into cardiomyocytes after cardiac stem or progenitor cell transplantation (163).

REGENERATIVE MEDICINE

Regenerative medicine is a branch of translational research aimed at replacing, engineering, and regenerating human cells, tissues, or organs so they regain normal function. In hepatology, observations show that several liver disorders can be treated with hepatocyte (HC) replacement instead of liver transplantation. As in any cell replacement procedure, it is crucial to follow up on the transplanted cells longitudinally.

NIS imaging has been used in HC transplantation by monitoring the cells after injection into a mouse model of hereditary tyrosinemia type 1. NIS-transduced HCs were transplanted into congenic fumarylacetoacetate hydrolase knockout mice, and this prevented liver failure. NIS-transduced HCs were imaged in vivo by SPECT for up to 85 days. This was the first noninvasive three-dimensional imaging of regenerating tissue in individual animals over time (164).

NIS imaging is also used to improve our understanding of (*a*) the in vivo behavior of mesoangioblasts, with the aim of using them as a regenerative therapy tool in muscular dystrophies, and (*b*) the effects of immunosuppressive therapies (e.g., cyclosporin A and costimulation-adhesion blockade therapy) on cell survival. Holvoet and colleagues (165) showed that costimulation-adhesion is clearly superior to cyclosporin A in reducing cell rejection. Costimulation-adhesion was mediated by a reduction in cytotoxic T cells and the upregulation of regulatory T cells.

CONCLUDING REMARKS AND FUTURE DIRECTIONS

NIS was used in clinical medicine to diagnose and treat thyroid disease for five decades before it was identified at the molecular level in 1996. Since its sequence was determined, significant progress has been made in understanding its tissue distribution and regulation, characterizing its structure/function relations, and using it as a reporter molecule. Fully elucidating the molecular mechanism by which NIS translocates its substrates will ultimately require determining the structure of NIS at atomic resolution—in different conformations and with its various substrates bound and not bound to it.

Acknowledgments

LITERATURE CITED

1. Baumann E. Über das Thyrojodin. Münch Med Wschr. 1896; 43:309–12.

2. Baumann E. Über den Jodgehalt der Schilddrusen von Menchen und Tieren. Hoppe-Seylers Z Physiol Chem. 1896; 22:1–17.

3. Hertz S, Roberts A, Means JH, Evans RD. Radioactive iodine as an indicator in thyroid physiology. J Pharmacol Exp Ther. 1940; 128:565–76.

4. Seidlin SM, Marinelli LD, Oshry E. Radioactive iodine therapy: effect on functioning metastases of adenocarcinoma of the thyroid. JAMA. 1946; 132:838–47.

5. Dai G, Levy O, Carrasco N. Cloning and characterization of the thyroid iodide transporter. Nature. 1996; 379:458–60. [PubMed: 8559252]

6. Eskandari S, Loo DD, Dai G, Levy O, Wright EM, Carrasco N. Thyroid Na^+/I^- symporter. Mechanism, stoichiometry, and specificity. J Biol Chem. 1997; 272:27230–38. [PubMed: 9341168]

7. Tazebay UH, Wapnir IL, Levy O, Dohán O, Zuckier LS, et al. The mammary gland iodide transporter is expressed during lactation and in breast cancer. Nat Med. 2000; 6:871–78. [PubMed: 10932223]

8. Wapnir IL, van de Rijn M, Nowels K, Amenta PS, Walton K, et al. Immunohistochemical profile of the sodium/iodide symporter in thyroid, breast, and other carcinomas using high density tissue microarrays and conventional sections. J Clin Endocrinol Metab. 2003; 88:1880–88. [PubMed: 12679487]

9. Paroder-Belenitsky M, Maestas MJ, Dohán O, Nicola JP, Reyna-Neyra A, et al. Mechanism of anion selectivity and stoichiometry of the Na^+/I^- symporter (NIS). PNAS. 2011; 108:17933–38. [PubMed: 22011571]

10. Dohán O, Portulano C, Basquin C, Reyna-Neyra A, Amzel LM, Carrasco N. The Na^+/I^- symporter (NIS) mediates electroneutral active transport of the environmental pollutant perchlorate. PNAS. 2007; 104:20250–55. [PubMed: 18077370]

11. Miller A, Russell SJ. The use of the NIS reporter gene for optimizing oncolytic virotherapy. Expert Opin Biol Ther. 2016; 16:15–32. [PubMed: 26457362]

12. Penheiter AR, Griesmann GE, Federspiel MJ, Dingli D, Russell SJ, Carlson SK. Pinhole micro-SPECT/CT for noninvasive monitoring and quantitation of oncolytic virus dispersion and percent infection in solid tumors. Gene Ther. 2012; 19:279–87. [PubMed: 21753796]

13. Bleichrodt, N., Born, MP. A meta-analysis of research on iodine and its relationship to cognitive development. In: Stanbury, JB., editor. The Damaged Brain of Iodine Deficiency. New York: Cognizant Comm; 1994. p. 195-200.

14. Portulano C, Paroder-Belenitsky M, Carrasco N. The Na^+/I^- symporter (NIS): mechanism and medical impact. Endocr Rev. 2014; 35:106–49. [PubMed: 24311738]

15. Bassett JH, Williams GR. Role of thyroid hormones in skeletal development and bone maintenance. Endocr Rev. 2016; 37:135–87. [PubMed: 26862888]

16. Videla LA, Fernández V, Cornejo P, Vargas R, Castillo I. Thyroid hormone in the frontier of cell protection, survival and functional recovery. Expert Rev Mol Med. 2015; 17:e10. [PubMed: 26004623]

17. Dunn JT, Delange F. Damaged reproduction: the most important consequence of iodine deficiency. J Clin Endocrinol Metab. 2001; 86:2360–63. [PubMed: 11397823]

18. Morreale de Escobar G, Obregón MJ, Escobar del Rey F. Is neuropsychological development related to maternal hypothyroidism or to maternal hypothyroxinemia? J Clin Endocrinol Metab. 2000; 85:3975–87. [PubMed: 11095417]

19. Verheesen RH, Schweitzer CM. Iodine deficiency, more than cretinism and goiter. Med Hypotheses. 2008; 71:645–48. [PubMed: 18703293]

20. Ivanova L, Zandberga E, Sili a K, Kalni a Z, Abols A, et al. Prognostic relevance of carbonic anhydrase IX expression is distinct in various subtypes of breast cancer and its silencing suppresses self-renewal capacity of breast cancer cells. Cancer Chemother Pharmacol. 2015; 75:235–46. [PubMed: 25422154]

21. World Health Org (WHO). Guideline: Fortification of Food-Grade Salt with Iodine for the Prevention and Control of Iodine Deficiency Disorders. Geneva: WHO; 2014.

22. Wolff J. Transport of iodide and other anions in the thyroid gland. Physiol Rev. 1964; 44:45–90. [PubMed: 14105583]

23. Smanik PA, Liu Q, Furminger TL, Ryu K, Xing S, et al. Cloning of the human sodium iodide symporter. Biochem Biophys Res Commun. 1996; 226:339–45. [PubMed: 8806637]

24. Smanik PA, Ryu KY, Theil KS, Mazzaferri EL, Jhiang SM. Expression, exon-intron organization, and chromosome mapping of the human sodium iodide symporter. Endocrinology. 1997; 138:3555–58. [PubMed: 9231811]

25. Levy O, Dai G, Riedel C, Ginter CS, Paul EM, et al. Characterization of the thyroid Na^+/I^- symporter with an anti-COOH terminus antibody. PNAS. 1997; 94:5568–73. [PubMed: 9159113]

26. Levy O, De la Vieja A, Carrasco N. The Na^+/I^- symporter (NIS): recent advances. J Bioenerg Biomembr. 1998; 30:195–206. [PubMed: 9672241]

27. Faham S, Watanabe A, Besserer GM, Cascio D, Specht A, et al. The crystal structure of a sodium galactose transporter reveals mechanistic insights into Na^+/sugar symport. Science. 2008; 321:810–14. [PubMed: 18599740]

28. Levy O, De la Vieja A, Ginter CS, Riedel C, Dai G, Carrasco N. N-linked glycosylation of the thyroid Na^+/I^- symporter (NIS). Implications for its secondary structure model. J Biol Chem. 1998; 273:22657–63. [PubMed: 9712895]

29. Li W, Nicola JP, Amzel LM, Carrasco N. Asn441 plays a key role in folding and function of the Na^+/I^- symporter (NIS). FASEB J. 2013; 27:3229–38. [PubMed: 23650190]

30. Nicola JP, Carrasco N, Mario Amzel L. Physiological sodium concentrations enhance the iodide affinity of the Na^+/I^- symporter. Nat Commun. 2014; 5:3948. [PubMed: 24888603]

31. Kogai T, Endo T, Saito T, Miyazaki A, Kawaguchi A, Onaya T. Regulation by thyroid-stimulating hormone of sodium/iodide symporter gene expression and protein levels in FRTL-5 cells. Endocrinology. 1997; 138:2227–32. [PubMed: 9165005]

32. Marcocci C, Cohen JL, Grollman EF. Effect of actinomycin D on iodide transport in FRTL-5 thyroid cells. Endocrinology. 1984; 115:2123–32. [PubMed: 6499763]

33. Riedel C, Levy O, Carrasco N. Post-transcriptional regulation of the sodium/iodide symporter by thyrotropin. J Biol Chem. 2001; 276:21458–63. [PubMed: 11290744]

34. Saito T, Endo T, Kawaguchi A, Ikeda M, Nakazato M. Increased expression of the Na^+/I^- symporter in cultured human thyroid cells exposed to thyrotropin and in Graves' thyroid tissue. J Clin Endocrinol Metab. 1997; 82:3331–36. [PubMed: 9329364]

35. Weiss SJ, Philp NJ, Grollman EF. Iodide transport in a continuous line of cultured cells from rat thyroid. Endocrinology. 1984; 114:1090–98. [PubMed: 6705729]

36. Carrasco, N. Thyroid hormones synthesis: thyroid iodide transport. In: Braverman, LE., Cooper, DS., editors. The Thyroide A Fundamental and Clinical Text. Philadelphia, PA: Lippincott Williams & Wilkins; 2013. p. 32-47.

37. Wolff J, Chaikoff IL. Plasma inorganic iodide as a homeostatic regulator of thyroid function. J Biol Chem. 1948; 174:555–64. [PubMed: 18865621]

38. Braverman LE, Ingbar SH. Changes in thyroidal function during adaptation to large doses of iodide. J Clin Investig. 1963; 42:1216–31. [PubMed: 14057854]

39. Leoni SG, Kimura ET, Santisteban P, De la Vieja A. Regulation of thyroid oxidative state by thioredoxin reductase has a crucial role in thyroid responses to iodide excess. Mol Endocrinol. 2011; 25:1924–35. [PubMed: 21903721]

40. Serrano-Nascimento C, Calil-Silveira J, Nunes MT. Posttranscriptional regulation of sodium-iodide symporter mRNA expression in the rat thyroid gland by acute iodide administration. Am J Physiol Cell Physiol. 2010; 298:C893–99. [PubMed: 20107044]

41. Vono-Toniolo J, Kopp P. Thyroglobulin gene mutations and other genetic defects associated with congenital hypothyroidism. Arq Bras Endocrinol Metabol. 2004; 48:70–82. [PubMed: 15611820]

42. Stratford AL, Boelaert K, Tannahill LA, Kim DS, Warfield A, et al. Pituitary tumor transforming gene binding factor: a novel transforming gene in thyroid tumorigenesis. J Clin Endocrinol Metab. 2005; 90:4341–49. [PubMed: 15886233]

43. Boelaert K, Smith VE, Stratford AL, Kogai T, Tannahill LA, et al. PTTG and PBF repress the human sodium iodide symporter. Oncogene. 2007; 26:4344–56. [PubMed: 17297475]

44. Lacoste C, Hervé J, Bou Nader M, Dos Santos A, Moniaux N, et al. Iodide transporter NIS regulates cancer cell motility and invasiveness by interacting with the Rho guanine nucleotide exchange factor LARG. Cancer Res. 2012; 72:5505–15. [PubMed: 22962269]

45. Roepke TK, King EC, Reyna-Neyra A, Paroder M, Purtell K, et al. *Kcne2* deletion uncovers its crucial role in thyroid hormone biosynthesis. Nat Med. 2009; 15:1186–94. [PubMed: 19767733]

46. Purtell K, Paroder-Belenitsky M, Reyna-Neyra A, Nicola JP, Koba W, et al. The KCNQ1-KCNE2 K^+ channel is required for adequate thyroid I^- uptake. FASEB J. 2012; 26:3252–59. [PubMed: 22549510]

47. Abbott GW, Tai KK, Neverisky DL, Hansler A, Hu Z, et al. KCNQ1, KCNE2, and Na^+-coupled solute transporters form reciprocally regulating complexes that affect neuronal excitability. Sci Signal. 2014; 7:ra22. [PubMed: 24595108]

48. Abbott GW. The KCNE2 K^+ channel regulatory subunit: ubiquitous influence, complex pathobiology. Gene. 2015; 569:162–72. [PubMed: 26123744]

49. Di Cosmo C, Fanelli G, Tonacchera M, Ferrarini E, Dimida A, et al. The sodium-iodide symporter expression in placental tissue at different gestational age: an immunohistochemical study. Clin Endocrinol. 2006; 65:544–48.

50. Mitchell AM, Manley SW, Morris JC, Powell KA, Bergert ER, Mortimer RH. Sodium iodide symporter (NIS) gene expression in human placenta. Placenta. 2001; 22:256–58. [PubMed: 11170832]

51. Morgenstern KE, Vadysirisack DD, Zhang Z, Cahill KV, Foster JA, et al. Expression of sodium iodide symporter in the lacrimal drainage system: implication for the mechanism underlying nasolacrimal duct obstruction in I131-treated patients. Ophthalmic Plast Reconstr Surg. 2005; 21:337–44.

52. Riesco-Eizaguirre G, Leoni SG, Mendiola M, Estevez-Cebrero MA, Gallego MI, et al. NIS mediates iodide uptake in the female reproductive tract and is a poor prognostic factor in ovarian cancer. J Clin Endocrinol Metab. 2014; 99:E1199–208. [PubMed: 24708099]

53. Spitzweg C, Dutton CM, Castro MR, Bergert ER, Goellner JR, et al. Expression of the sodium iodide symporter in human kidney. Kidney Int. 2001; 59:1013–23. [PubMed: 11231356]

54. Marti-Climent JM, Collantes M, Jauregui-Osoro M, Quincoces G, Prieto E, et al. Radiation dosimetry and biodistribution in non-human primates of the sodium/iodide PET ligand [^{18}F]-tetrafluoroborate. EJNMMI Res. 2015; 5:70. [PubMed: 26635227]

55. Akturk M, Oruc AS, Danisman N, Erkek S, Buyukkagnici U, et al. Na^+/I^- symporter and type 3 iodothyronine deiodinase gene expression in amniotic membrane and placenta and its relationship to maternal thyroid hormones. Biol Trace Element Res. 2013; 154:338–44.

56. Altorjay A, Dohán O, Szilágyi A, Paroder M, Wapnir IL, Carrasco N. Expression of the Na^+/I^- symporter (NIS) is markedly decreased or absent in gastric cancer and intestinal metaplastic mucosa of Barrett esophagus. BMC Cancer. 2007; 7:5. [PubMed: 17214887]

57. La Perle KM, Kim DC, Hall NC, Bobbey A, Shen DH, et al. Modulation of sodium/iodide symporter expression in the salivary gland. Thyroid. 2013; 23:1029–36. [PubMed: 23441638]

58. Spitzweg C, Joba W, Morris JC, Heufelder AE. Regulation of sodium iodide symporter gene expression in FRTL-5 rat thyroid cells. Thyroid. 1999; 9:821–30. [PubMed: 10482376]

59. Dagogo-Jack S. Dietary iodine affects epidermal growth factor levels in mouse thyroid and sub-maxillary glands. Endocr Res. 1994; 20:247–57. [PubMed: 7995255]

60. Geiszt M, Witta J, Baffi J, Lekstrom K, Leto TL. Dual oxidases represent novel hydrogen peroxide sources supporting mucosal surface host defense. FASEB J. 2003; 17:1502–4. [PubMed: 12824283]

61. Gupta A, Lakhoo K, Pritchard N, Herbert M. Epidermal growth factor in neonatal saliva. Eur J Pediatr Surg. 2008; 18:245–48. [PubMed: 18629765]

62. Venturi S, Venturi M. Iodine in evolution of salivary glands and in oral health. Nutr Health. 2009; 20:119–34. [PubMed: 19835108]

63. Nicola JP, Basquin C, Portulano C, Reyna-Neyra A, Paroder M, Carrasco N. The Na$^+$/I$^-$ symporter mediates active iodide uptake in the intestine. Am J Physiol Cell Physiol. 2009; 296:C654–62. [PubMed: 19052257]

64. Nicola JP, Carrasco N, Masini-Repiso AM. Dietary I$^-$ absorption: expression and regulation of the Na$^+$/I$^-$ symporter in the intestine. Vitam Horm. 2015; 98:1–31. [PubMed: 25817864]

65. Vejbjerg P, Knudsen N, Perrild H, Laurberg P, Andersen S, et al. Estimation of iodine intake from various urinary iodine measurements in population studies. Thyroid. 2009; 19:1281–86. [PubMed: 19888863]

66. Scott DA, Wang R, Kreman TM, Sheffield VC, Karniski LP. The Pendred syndrome gene encodes a chloride-iodide transport protein. Nat Genet. 1999; 21:440–43. [PubMed: 10192399]

67. van den Hove MF, Croizet-Berger K, Jouret F, Guggino SE, Guggino WB, et al. The loss of the chloride channel, ClC-5, delays apical iodide efflux and induces a euthyroid goiter in the mouse thyroid gland. Endocrinology. 2006; 147:1287–96. [PubMed: 16306076]

68. Calebiro D, Porazzi P, Bonomi M, Lisi S, Grindati A, et al. Absence of primary hypothyroidism and goiter in *Slc26a4* (−/−) mice fed on a low iodine diet. J Endocrinol Investig. 2011; 34:593–98. [PubMed: 20834201]

69. Iwata T, Yoshida T, Teranishi M, Murata Y, Hayashi Y, et al. Influence of dietary iodine deficiency on the thyroid gland in *Slc26a4*-null mutant mice. Thyroid Res. 2011; 4:10. [PubMed: 21689387]

70. Cho JY, Xing S, Liu X, Buckwalter TL, Hwa L, et al. Expression and activity of human Na$^+$/I$^-$ symporter in human glioma cells by adenovirus-mediated gene delivery. Gene Ther. 2000; 7:740–49. [PubMed: 10822300]

71. Renier C, Vogel H, Offor O, Yao C, Wapnir I. Breast cancer brain metastases express the sodium iodide symporter. J Neurooncol. 2010; 96:331–36. [PubMed: 19618116]

72. Wapnir IL, Goris M, Yudd A, Dohán O, Adelman D, et al. The Na$^+$/I$^-$ symporter mediates iodide uptake in breast cancer metastases and can be selectively down-regulated in the thyroid. Clin Cancer Res. 2004; 10:4294–302. [PubMed: 15240514]

73. Kogai T, Curcio F, Hyman S, Cornford EM, Brent GA, Hershman JM. Induction of follicle formation in long-term cultured normal human thyroid cells treated with thyrotropin stimulates iodide uptake but not sodium/iodide symporter messenger RNA and protein expression. J Endocrinol. 2000; 167:125–35. [PubMed: 11018760]

74. Kogai T, Brent GA. The sodium iodide symporter (NIS): regulation and approaches to targeting for cancer therapeutics. Pharmacol Ther. 2012; 135:355–70. [PubMed: 22750642]

75. Kogai T, Kanamoto Y, Li AI, Che LH, Ohashi E, et al. Differential regulation of sodium/iodide symporter gene expression by nuclear receptor ligands in MCF-7 breast cancer cells. Endocrinology. 2005; 146:3059–69. [PubMed: 15817668]

76. Unterholzner S, Willhauck MJ, Cengic N, Schütz M, Göke B, et al. Dexamethasone stimulation of retinoic acid-induced sodium iodide symporter expression and cytotoxicity of 131-I in breast cancer cells. J Clin Endocrinol Metab. 2006; 91:69–78. [PubMed: 16234306]

77. Dohán O, De la Vieja A, Carrasco N. Hydrocortisone and purinergic signaling stimulate sodium/iodide symporter (NIS)-mediated iodide transport in breast cancer cells. Mol Endocrinol. 2006; 20:1121–37. [PubMed: 16439463]

78. Kogai T, Kanamoto Y, Che LH, Taki K, Moatamed F, et al. Systemic retinoic acid treatment induces sodium/iodide symporter expression and radioiodide uptake in mouse breast cancer models. Cancer Res. 2004; 64:415–22. [PubMed: 14729653]

79. Brown-Grant K. The metabolism of iodide by the thyroid gland and by the uterus during early pregnancy in the rat. J Physiol. 1965; 176:73–90. [PubMed: 14281408]

80. Trovato M, Vitarelli E, Tripepi M, Abate A, Rizzo P, et al. Expression of NA-1 symporter (NIS) in endometrial mucosa of fertile, sterile and post-menopausal women. Histol Histopathol. 2008; 23:549–54. [PubMed: 18283639]

81. Lacroix L, Mian C, Caillou B, Talbot M, Filetti S, et al. Na$^+$/I$^-$ symporter and Pendred syndrome gene and protein expressions in human extra-thyroidal tissues. Eur J Endocrinol. 2001; 144:297–302. [PubMed: 11248751]

82. Spitzweg C, Joba W, Eisenmenger W, Heufelder AE. Analysis of human sodium iodide symporter gene expression in extrathyroidal tissues and cloning of its complementary deoxyribonucleic acids from salivary gland, mammary gland, and gastric mucosa. J Clin Endocrinol Metab. 1998; 83:1746–51. [PubMed: 9589686]

83. Chaffin CL, Vandevoort CA. Follicle growth, ovulation, and luteal formation in primates and rodents: a comparative perspective. Exp Biol Med. 2013; 238:539–48.

84. Am. Acad. Pediatr.; Rose SR, Am. Thyroid Assoc.; Brown RS, Lawson Wilkins Pediatr. Endocr. Soc. Update of newborn screening and therapy for congenital hypothyroidism. Pediatrics. 2006; 117:2290–303. [PubMed: 16740880]

85. Park SM, Chatterjee VK. Genetics of congenital hypothyroidism. J Med Genet. 2005; 42:379–89. [PubMed: 15863666]

86. Clifton-Bligh RJ, Wentworth JM, Heinz P, Crisp MS, John R, et al. Mutation of the gene encoding human TTF-2 associated with thyroid agenesis, cleft palate and choanal atresia. Nat Genet. 1998; 19:399–401. [PubMed: 9697705]

87. Dentice M, Cordeddu V, Rosica A, Ferrara AM, Santarpia L, et al. Missense mutation in the transcription factor NKX2-5: a novel molecular event in the pathogenesis of thyroid dysgenesis. J Clin Endocrinol Metab. 2006; 91:1428–33. [PubMed: 16418214]

88. Krude H, Schutz B, Biebermann H, von Moers A, Schnabel D, et al. Choreoathetosis, hypothyroidism, and pulmonary alterations due to human NKX2-1 haploinsufficiency. J Clin Investig. 2002; 109:475–80. [PubMed: 11854319]

89. Macchia PE, Lapi P, Krude H, Pirro MT, Missero C, et al. PAX8 mutations associated with congenital hypothyroidism caused by thyroid dysgenesis. Nat Genet. 1998; 19:83–86. [PubMed: 9590296]

90. Pohlenz J, Dumitrescu A, Zundel D, Martiné U, Schönberger W, et al. Partial deficiency of thyroid transcription factor 1 produces predominantly neurological defects in humans and mice. J Clin Investig. 2002; 109:469–73. [PubMed: 11854318]

91. Avbelj M, Tahirovic H, Debeljak M, Kusekova M, Toromanovic A, et al. High prevalence of thyroid peroxidase gene mutations in patients with thyroid dyshormonogenesis. Eur J Endocrinol. 2007; 156:511–19. [PubMed: 17468186]

92. Bizhanova A, Kopp P. Genetics and phenomics of Pendred syndrome. Mol Cell Endocrinol. 2010; 322:83–90. [PubMed: 20298745]

93. Gutnisky VJ, Moya CM, Rivolta CM, Domené S, Varela V, et al. Two distinct compound heterozygous constellations (R277X/IVS34-1G>C and R277X/R1511X) in the thyroglobulin (TG) gene in affected individuals of a Brazilian kindred with congenital goiter and defective TG synthesis. J Clin Endocrinol Metab. 2004; 89:646–57. [PubMed: 14764776]

94. Moreno JC, Bikker H, Kempers MJ, van Trotsenburg AS, Baas F, et al. Inactivating mutations in the gene for thyroid oxidase 2 (THOX2) and congenital hypothyroidism. N Engl J Med. 2002; 347:95–102. [PubMed: 12110737]

95. Moreno JC, Klootwijk W, van Toor H, Pinto G, D'Alessandro M, et al. Mutations in the iodotyrosine deiodinase gene and hypothyroidism. N Engl J Med. 2008; 358:1811–18. [PubMed: 18434651]

96. Pohlenz J, Refetoff S. Mutations in the sodium/iodide symporter (NIS) gene as a cause for iodide transport defects and congenital hypothyroidism. Biochimie. 1999; 81:469–76. [PubMed: 10403177]

97. Reed-Tsur MD, De la Vieja A, Ginter CS, Carrasco N. Molecular characterization of V59E NIS, a Na^+/I^- symporter mutant that causes congenital I- transport defect. Endocrinology. 2008; 149:3077–84. [PubMed: 18339708]

98. Paroder V, Nicola JP, Ginter CS, Carrasco N. The iodide-transport-defect-causing mutation R124H: a delta-amino group at position 124 is critical for maturation and trafficking of the Na^+/I^- symporter. J Cell Sci. 2013; 126:3305–13. [PubMed: 23690546]

99. Kosugi S, Okamoto H, Tamada A, Sanchez-Franco F. A novel peculiar mutation in the sodium/iodide symporter gene in Spanish siblings with iodide transport defect. J Clin Endocrinol Metab. 2002; 87:3830–36. [PubMed: 12161518]

100. De La Vieja A, Ginter CS, Carrasco N. The Q267E mutation in the sodium/iodide symporter (NIS) causes congenital iodide transport defect (ITD) by decreasing the NIS turnover number. J Cell Sci. 2004; 117:677–87. [PubMed: 14734652]

101. Nicola JP, Reyna-Neyra A, Saenger P, Rodriguez-Buritica DF, Godoy JD, et al. The sodium/iodide symporter mutant V270E causes stunted growth but no cognitive deficiency. J Clin Endocrinol Metab. 2015; 100:E1353–61. [PubMed: 26204134]

102. Montanelli L, Agretti P, Marco G, Bagattini B, Ceccarelli C, et al. Congenital hypothyroidism and late-onset goiter: identification and characterization of a novel mutation in the sodium/iodide symporter of the proband and family members. Thyroid. 2009; 19:1419–25. [PubMed: 19916865]

103. De la Vieja A, Reed MD, Ginter CS, Carrasco N. Amino acid residues in transmembrane segment IX of the Na$^+$/I$^-$ symporter play a role in its Na$^+$ dependence and are critical for transport activity. J Biol Chem. 2007; 282:25290–98. [PubMed: 17606623]

104. Levy O, Ginter CS, De la Vieja A, Levy D, Carrasco N. Identification of a structural requirement for thyroid Na$^+$/I$^-$ symporter (NIS) function from analysis of a mutation that causes human congenital hypothyroidism. FEBS Lett. 1998; 429:36–40. [PubMed: 9657379]

105. Dohán O, Gavrielides MV, Ginter C, Amzel LM, Carrasco N. Na$^+$/I$^-$ symporter activity requires a small and uncharged amino acid residue at position 395. Mol Endocrinol. 2002; 16:1893–902. [PubMed: 12145342]

106. Li W, Nicola JP, Amzel LM, Carrasco N. Asn441 plays a key role in folding and function of the Na$^+$/I$^-$ symporter (NIS). FASEB J. 2013; 27:3229–38. [PubMed: 23650190]

107. De la Vieja A, Ginter CS, Carrasco N. Molecular analysis of a congenital iodide transport defect: G543E impairs maturation and trafficking of the Na$^+$/I$^-$ symporter. Mol Endocrinol. 2005; 19:2847–58. [PubMed: 15976004]

108. Portulano C, Paroder-Belenitsky M, Carrasco N. The Na$^+$/I$^-$ symporter (NIS): mechanism and medical impact. Endocr Rev. 2014; 35:106–49. [PubMed: 24311738]

109. Nicola JP, Nazar M, Serrano-Nascimento C, Goulart-Silva F, Sobrero G, et al. Iodide transport defect: functional characterization of a novel mutation in the Na$^+$/I$^-$ symporter 5′-untranslated region in a patient with congenital hypothyroidism. J Clin Endocrinol Metab. 2011; 96:E1100–7. [PubMed: 21565787]

110. Yamashita A, Singh SK, Kawate T, Jin Y, Gouaux E. Crystal structure of a bacterial homologue of Na$^+$/Cl$^-$-dependent neurotransmitter transporters. Nature. 2005; 437:215–23. [PubMed: 16041361]

111. Khafizov K, Perez C, Koshy C, Quick M, Fendler K, et al. Investigation of the sodium-binding sites in the sodium-coupled betaine transporter BetP. PNAS. 2012; 109:E3035–44. [PubMed: 23047697]

112. Weyand S, Shimamura T, Yajima S, Suzuki S, Mirza O, et al. Structure and molecular mechanism of a nucleobase-cation-symport-1 family transporter. Science. 2008; 322:709–13. [PubMed: 18927357]

113. Ravera S, Quick M, Nicola JP, Carrasco N, Amzel LM. Beyond non-integer Hill coefficients: a novel approach to analyzing binding data, applied to Na$^+$-driven transporters. J Gen Physiol. 2015; 145:555–63. [PubMed: 26009546]

114. Zhao C, Stolzenberg S, Gracia L, Weinstein H, Noskov S, Shi L. Ion-controlled conformational dynamics in the outward-open transition from an occluded state of LeuT. Biophys J. 2012; 103:878–88. [PubMed: 23009837]

115. Loo DD, Jiang X, Gorraitz E, Hirayama BA, Wright EM. Functional identification and characterization of sodium binding sites in Na symporters. PNAS. 2013; 110:E4557–66. [PubMed: 24191006]

116. Meinild AK, Forster IC. Using lithium to probe sequential cation interactions with GAT1. Am J Physiol Cell Physiol. 2012; 302:C1661–75. [PubMed: 22460712]

117. Paroder V, Nicola JP, Ginter CS, Carrasco N. The iodide transport defect-causing mutation R124H: a delta-amino group at position 124 is critical for maturation and trafficking of the Na$^+$/I$^-$ symporter (NIS). J Cell Sci. 2013; 126:3305–13. [PubMed: 23690546]

118. Shimura H, Haraguchi K, Miyazaki A, Endo T, Onaya T. Iodide uptake and experimental 131I therapy in transplanted undifferentiated thyroid cancer cells expressing the Na$^+$/I$^-$ symporter gene. Endocrinology. 1997; 138:4493–96. [PubMed: 9322970]

119. Baril P, Martin-Duque P, Vassaux G. Visualization of gene expression in the live subject using the Na/I symporter as a reporter gene: applications in biotherapy. Br J Pharmacol. 2010; 159:761–71. [PubMed: 19814733]

120. Boland A, Ricard M, Opolon P, Bidart JM, Yeh P, et al. Adenovirus-mediated transfer of the thyroid sodium/iodide symporter gene into tumors for a targeted radiotherapy. Cancer Res. 2000; 60:3484–92. [PubMed: 10910060]

121. Penheiter AR, Russell SJ, Carlson SK. The sodium iodide symporter (NIS) as an imaging reporter for gene, viral, and cell-based therapies. Curr Gene Ther. 2012; 12:33–47. [PubMed: 22263922]

122. Spitzweg C, Dietz AB, O'Connor MK, Bergert ER, Tindall DJ, et al. In vivo sodium iodide symporter gene therapy of prostate cancer. Gene Ther. 2001; 8:1524–31. [PubMed: 11704812]

123. Spitzweg C, Heufelder AE, Morris JC. Thyroid iodine transport. Thyroid. 2000; 10:321–30. [PubMed: 10807060]

124. Hingorani M, Spitzweg C, Vassaux G, Newbold K, Melcher A, et al. The biology of the sodium iodide symporter and its potential for targeted gene delivery. Curr Cancer Drug Targets. 2010; 10:242–67. [PubMed: 20201784]

125. Spitzweg C, Morris JC. Gene therapy for thyroid cancer: current status and future prospects. Thyroid. 2004; 14:424–34. [PubMed: 15242569]

126. Niu G, Gaut AW, Ponto LL, Hichwa RD, Madsen MT, et al. Multimodality noninvasive imaging of gene transfer using the human sodium iodide symporter. J Nucl Med. 2004; 45:445–49. [PubMed: 15001685]

127. Msaouel P, Iankov ID, Allen C, Aderca I, Federspiel MJ, et al. Noninvasive imaging and radiovirotherapy of prostate cancer using an oncolytic measles virus expressing the sodium iodide symporter. Mol Ther. 2009; 17:2041–48. [PubMed: 19773744]

128. Peerlinck I, Merron A, Baril P, Conchon S, Martin-Duque P, et al. Targeted radionuclide therapy using a Wnt-targeted replicating adenovirus encoding the Na/I symporter. Clin Cancer Res. 2009; 15:6595–601. [PubMed: 19861465]

129. Haddad D, Zanzonico PB, Carlin S, Chen CH, Chen NG, et al. A vaccinia virus encoding the human sodium iodide symporter facilitates long-term image monitoring of virotherapy and targeted radiotherapy of pancreatic cancer. J Nucl Med. 2012; 53:1933–42. [PubMed: 23139088]

130. Russell SJ, Federspiel MJ, Peng KW, Tong C, Dingli D, et al. Remission of disseminated cancer after systemic oncolytic virotherapy. Mayo Clin Proc. 2014; 89:926–33. [PubMed: 24835528]

131. Li H, Peng KW, Dingli D, Kratzke RA, Russell SJ. Oncolytic measles viruses encoding interferon beta and the thyroidal sodium iodide symporter gene for mesothelioma virotherapy. Cancer Gene Ther. 2010; 17:550–58. [PubMed: 20379224]

132. Dwyer RM, Bergert ER, O'Connor MK, Gendler SJ, Morris JC. In vivo radioiodide imaging and treatment of breast cancer xenografts after MUC1-driven expression of the sodium iodide symporter. Clin Cancer Res. 2005; 11:1483–89. [PubMed: 15746050]

133. Dwyer RM, Bergert ER, O'Connor MK, Gendler SJ, Morris JC. Adenovirus-mediated and targeted expression of the sodium-iodide symporter permits in vivo radioiodide imaging and therapy of pancreatic tumors. Hum Gene Ther. 2006; 17:661–68. [PubMed: 16776574]

134. Dwyer RM, Bergert ER, O'Connor MK, Gendler SJ, Morris JC. Sodium iodide symporter-mediated radioiodide imaging and therapy of ovarian tumor xenografts in mice. Gene Ther. 2006; 13:60–66. [PubMed: 16121204]

135. Dwyer RM, Schatz SM, Bergert ER, Myers RM, Harvey ME, et al. A preclinical large animal model of adenovirus-mediated expression of the sodium-iodide symporter for radioiodide imaging and therapy of locally recurrent prostate cancer. Mol Ther. 2005; 12:835–41. [PubMed: 16054438]

136. Trujillo MA, Oneal MJ, Davydova J, Bergert E, Yamamoto M, Morris JC 3rd. Construction of an MUC-1 promoter driven, conditionally replicating adenovirus that expresses the sodium iodide symporter for gene therapy of breast cancer. Breast Cancer Res. 2009; 11:R53. [PubMed: 19635153]

137. Trujillo MA, Oneal MJ, McDonough S, Qin R, Morris JC. A probasin promoter, conditionally replicating adenovirus that expresses the sodium iodide symporter (NIS) for radiovirotherapy of prostate cancer. Gene Ther. 2010; 17:1325–32. [PubMed: 20428214]

138. Naik S, Russell SJ. Engineering oncolytic viruses to exploit tumor specific defects in innate immune signaling pathways. Expert Opin Biol Ther. 2009; 9:1163–76. [PubMed: 19637971]

139. Peng KW, Ahmann GJ, Pham L, Greipp PR, Cattaneo R, Russell SJ. Systemic therapy of myeloma xenografts by an attenuated measles virus. Blood. 2001; 98:2002–7. [PubMed: 11567982]

140. Galanis E, Atherton PJ, Maurer MJ, Knutson KL, Dowdy SC, et al. Oncolytic measles virus expressing the sodium iodide symporter to treat drug-resistant ovarian cancer. Cancer Res. 2015; 75:22–30. [PubMed: 25398436]

141. Blechacz B, Splinter PL, Greiner S, Myers R, Peng KW, et al. Engineered measles virus as a novel oncolytic viral therapy system for hepatocellular carcinoma. Hepatology. 2006; 44:1465–77. [PubMed: 17133484]

142. Domingo-Musibay E, Allen C, Kurokawa C, Hardcastle JJ, Aderca I, et al. Measles Edmonston vaccine strain derivatives have potent oncolytic activity against osteosarcoma. Cancer Gene Ther. 2014; 21:483–90. [PubMed: 25394505]

143. Li H, Peng KW, Russell SJ. Oncolytic measles virus encoding thyroidal sodium iodide symporter for squamous cell cancer of the head and neck radiovirotherapy. Hum Gene Ther. 2012; 23:295–301. [PubMed: 22235810]

144. Liu YP, Wang J, Avanzato VA, Bakkum-Gamez JN, Russell SJ, et al. Oncolytic vaccinia virotherapy for endometrial cancer. Gynecol Oncol. 2014; 132:722–29. [PubMed: 24434058]

145. Haddad D, Chen CH, Carlin S, Silberhumer G, Chen NG, et al. Imaging characteristics, tissue distribution, and spread of a novel oncolytic vaccinia virus carrying the human sodium iodide symporter. PLOS ONE. 2012; 7:e41647. [PubMed: 22912675]

146. Haddad D, Chen NG, Zhang Q, Chen CH, Yu YA, et al. Insertion of the human sodium iodide symporter to facilitate deep tissue imaging does not alter oncolytic or replication capability of a novel vaccinia virus. J Transl Med. 2011; 9:36. [PubMed: 21453532]

147. Belin LJ, Ady JW, Lewis C, Marano D, Gholami S, et al. An oncolytic vaccinia virus expressing the human sodium iodine symporter prolongs survival and facilitates SPECT/CT imaging in an orthotopic model of malignant pleural mesothelioma. Surgery. 2013; 154:486–95. [PubMed: 23890748]

148. Jun KH, Gholami S, Song TJ, Au J, Haddad D, et al. A novel oncolytic viral therapy and imaging technique for gastric cancer using a genetically engineered vaccinia virus carrying the human sodium iodide symporter. J Exp Clin Cancer Res. 2014; 33:2. [PubMed: 24383569]

149. Eveno C, Mojica K, Ady JW, Thorek DL, Longo V, et al. Gene therapy using therapeutic and diagnostic recombinant oncolytic vaccinia virus GLV-1h153 for management of colorectal peritoneal carcinomatosis. Surgery. 2015; 157:331–37. [PubMed: 25616946]

150. Gholami S, Chen CH, Belin LJ, Lou E, Fujisawa S, et al. Vaccinia virus GLV-1h153 is a novel agent for detection and effective local control of positive surgical margins for breast cancer. Breast Cancer Res. 2013; 15:R26. [PubMed: 23506710]

151. Gholami S, Haddad D, Chen CH, Chen NG, Zhang Q, et al. Novel therapy for anaplastic thyroid carcinoma cells using an oncolytic vaccinia virus carrying the human sodium iodide symporter. Surgery. 2011; 150:1040–47. [PubMed: 22136819]

152. Mansfield DC, Kyula JN, Rosenfelder N, Chao-Chu J, Kramer-Marek G, et al. Oncolytic vaccinia virus as a vector for therapeutic sodium iodide symporter gene therapy in prostate cancer. Gene Ther. 2016; 23:357–68. [PubMed: 26814609]

153. Lehner S, Lang C, Kaissis G, Todica A, Zacherl MJ, et al. [124]I-PET assessment of human sodium iodide symporter reporter gene activity for highly sensitive in vivo monitoring of teratoma formation in mice. Mol Imaging Biol. 2015; 17:874–83. [PubMed: 25896817]

154. Knoop K, Schwenk N, Schmohl K, Müller A, Zach C, et al. Mesenchymal stem cell-mediated, tumor stroma-targeted radioiodine therapy of metastatic colon cancer using the sodium iodide symporter as theranostic gene. J Nucl Med. 2015; 56:600–6. [PubMed: 25745085]

155. Park JW, Jung KH, Lee JH, Moon SH, Cho YS, et al. Imaging early fate of cancer stem cells in mouse hindlimbs with sodium iodide symporter gene and I-124 PET. Mol Imaging Biol. 2016; 18:748. [PubMed: 26914278]

156. Micci MA, Boone DR, Parsley MA, Wei J, Patrikeev I, et al. Development of a novel imaging system for cell therapy in the brain. Stem Cell Res Ther. 2015; 6:131. [PubMed: 26194790]

157. Terrovitis J, Kwok KF, Lautamaki R, Engles JM, Barth AS, et al. Ectopic expression of the sodium-iodide symporter enables imaging of transplanted cardiac stem cells in vivo by single-photon emission computed tomography or positron emission tomography. J Am Coll Cardiol. 2008; 52:1652–60. [PubMed: 18992656]

158. Templin C, Zweigerdt R, Schwanke K, Olmer R, Ghadri JR, et al. Transplantation and tracking of human-induced pluripotent stem cells in a pig model of myocardial infarction: assessment of cell survival, engraftment, and distribution by hybrid single photon emission computed tomography/ computed tomography of sodium iodide symporter transgene expression. Circulation. 2012; 126:430–39. [PubMed: 22767659]

159. Lee AR, Woo SK, Kang SK, Lee SY, Lee MY, et al. Adenovirus-mediated expression of human sodium-iodide symporter gene permits in vivo tracking of adipose tissue-derived stem cells in a canine myocardial infarction model. Nucl Med Biol. 2015; 42:621–29. [PubMed: 25899941]

160. Shi S, Zhang M, Guo R, Miao Y, Zhang M, et al. Feasibility of lentiviral-mediated sodium iodide symporter gene delivery for the efficient monitoring of bone marrow-derived mesenchymal stem cell transplantation and survival. Int J Mol Med. 2014; 34:1547–54. [PubMed: 25319483]

161. Shi S, Zhang M, Guo R, Miao Y, Zhang X, Li B. Molecular imaging to monitor repair of myocardial infarction using genetically engineered bone marrow-derived mesenchymal stem cells. Curr Gene Ther. 2015; 15:460–71. [PubMed: 25892408]

162. Chang C, Chan A, Lin X, Higuchi T, Terrovitis J, et al. Cellular bioenergetics is an important determinant of the molecular imaging signal derived from luciferase and the sodium-iodide symporter. Circ Res. 2013; 112:441–50. [PubMed: 23255420]

163. Kang JH, Lee DS, Paeng JC, Lee JS, Kim YH, et al. Development of a sodium/iodide symporter (NIS)-transgenic mouse for imaging of cardiomyocyte-specific reporter gene expression. J Nucl Med. 2005; 46:479–83. [PubMed: 15750162]

164. Hickey RD, Mao SA, Amiot B, Suksanpaisan L, Miller A, et al. Noninvasive 3-dimensional imaging of liver regeneration in a mouse model of hereditary tyrosinemia type 1 using the sodium iodide symporter gene. Liver Transpl. 2015; 21:442–53. [PubMed: 25482651]

165. Holvoet B, Quattrocelli M, Belderbos S, Pollaris L, Wolfs E, et al. Sodium iodide symporter PET and BLI noninvasively reveal mesoangioblast survival in dystrophic mice. Stem Cell Rep. 2015; 5:1183–95.
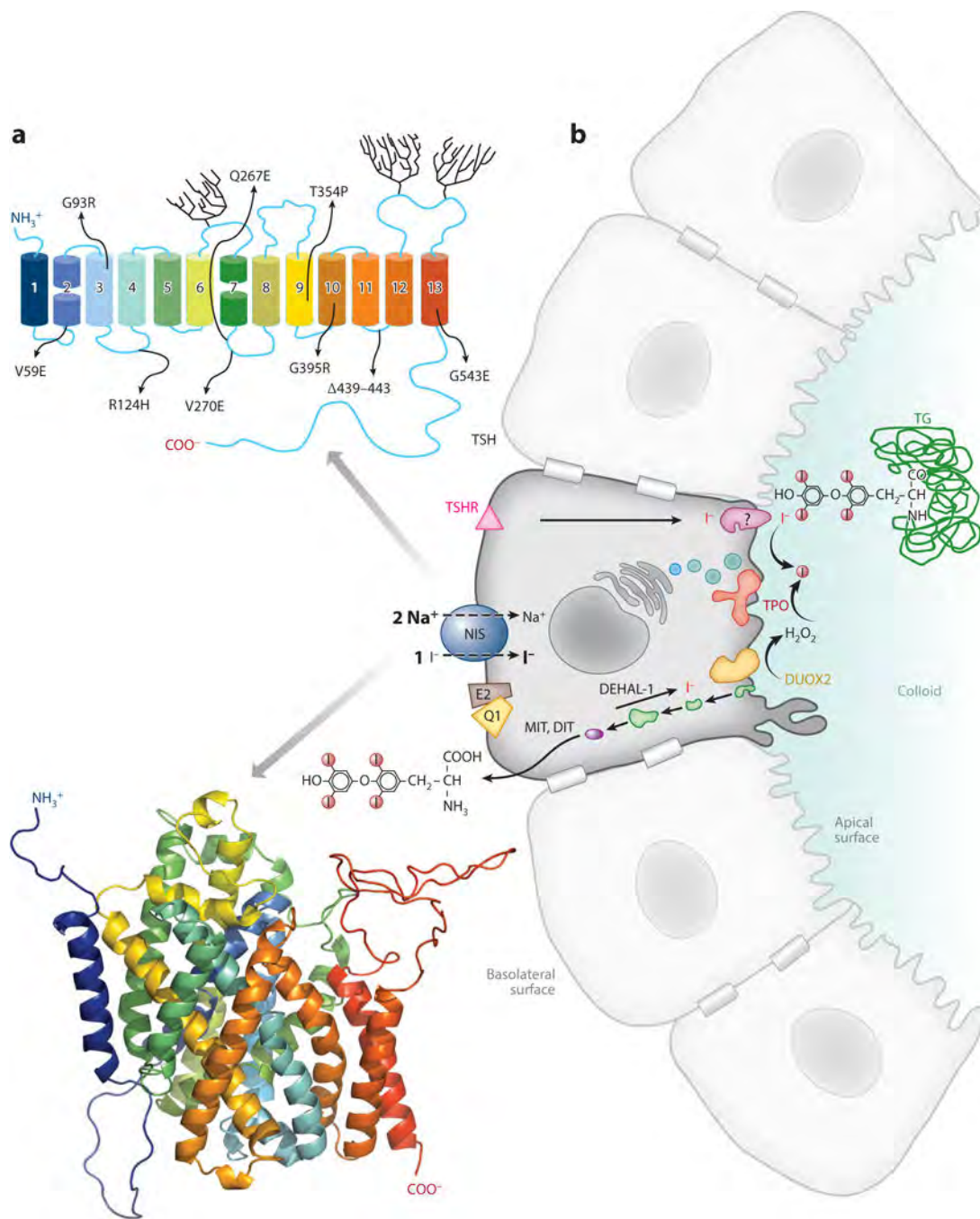
Figure 1.

Schematic representation of TH biogenesis. (*a*) Experimentally tested NIS secondary structure model (*upper left*). TMSs are represented by cylinders of different colors, which match those used in the depiction of the current NIS homology model (*lower left*) based on the crystal structure of vSGLT. Blue lines represent extracellular and intracellular segments, and branches represent N-linked glycosylation sites (N225, 489, and 502). NIS mutations identified in patients with ITD and studied at the molecular level by investigating the effects of different amino acid substitutions at the relevant positions are named using the single-

letter amino acid code.   indicates deletions. (*b*) Schematic representation of thyroid hormone biogenesis: NIS (*blue*), TG (*green*), TPO (*red*), DUOX2 (*yellow*), and KCNQ1-KCNE2 potassium channel (*yellow and brown* at the basolateral surface structures). Abbreviations: DEHAL-1, dehalogenase 1; DIT, 3,5-di-iodotyrosine; DUOX2, dual oxidase 2; ITD, I⁻ transport defect; MIT, 3-mono-iodotyrosine; NIS, Na$^+$/I$^-$ symporter; TG, thyroglobulin; TH, thyroid hormone; TMS, transmembrane segment; TPO, thyroid peroxidase; TSH, thyroid-stimulating hormone; TSHR, TSH receptor; vSGLT, *Vibrio parahaemolyticus* Na$^+$/galactose transporter.
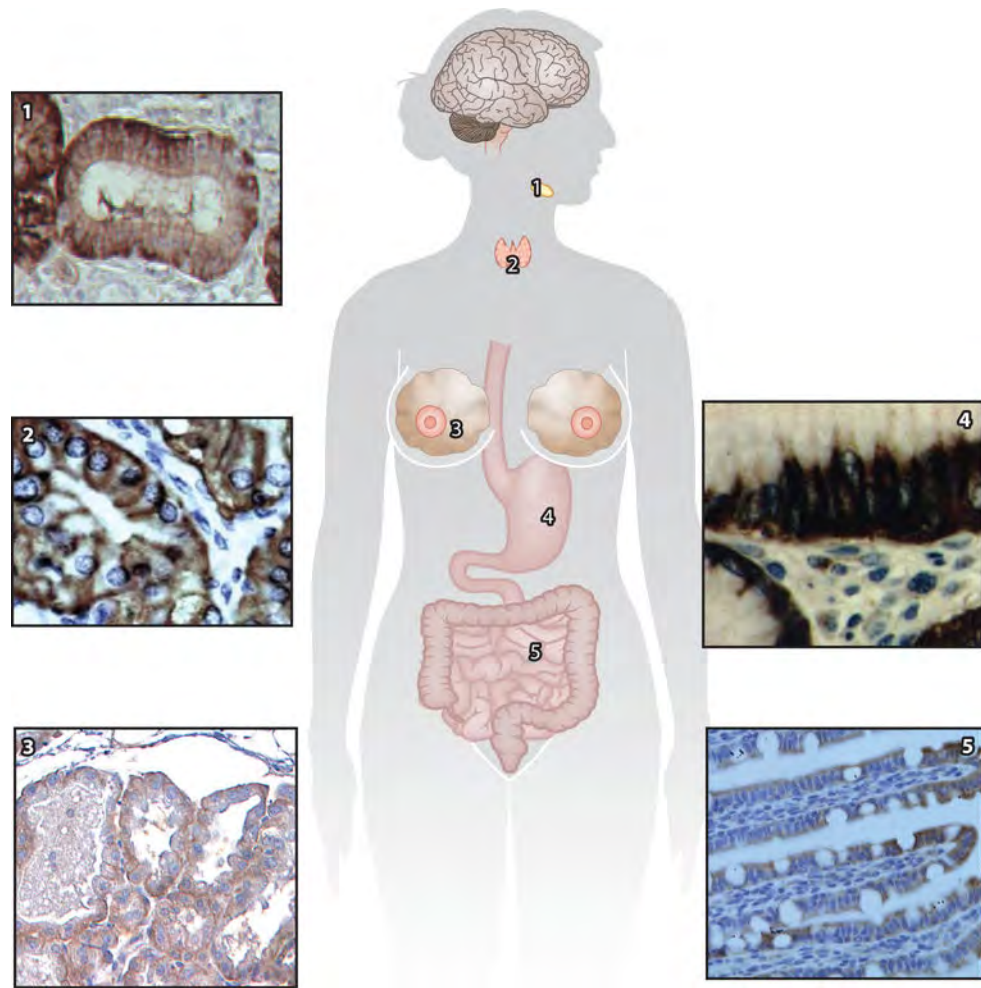
Figure 2.
NIS expression in the thyroid and extrathyroidal tissues. NIS expression in tissues that actively transport I⁻ was detected by IHC using affinity-purified anti-NIS antibodies. Epithelial cells from (1) salivary gland, (2) Graves' thyroid, (3) gestational breast, and (4) stomach show basolateral expression; by contrast, (5) intestine epithelial cells show apical localization. Images shown at magnifications of × 40 (3), ×60 (2, 5), and ×100 (1, 4). Images 2 and 4 are adapted from Reference 56, and image 5 is adapted from Reference 63. Abbreviations: IHC, immunohistochemistry; NIS, Na^+/I^- symporter.
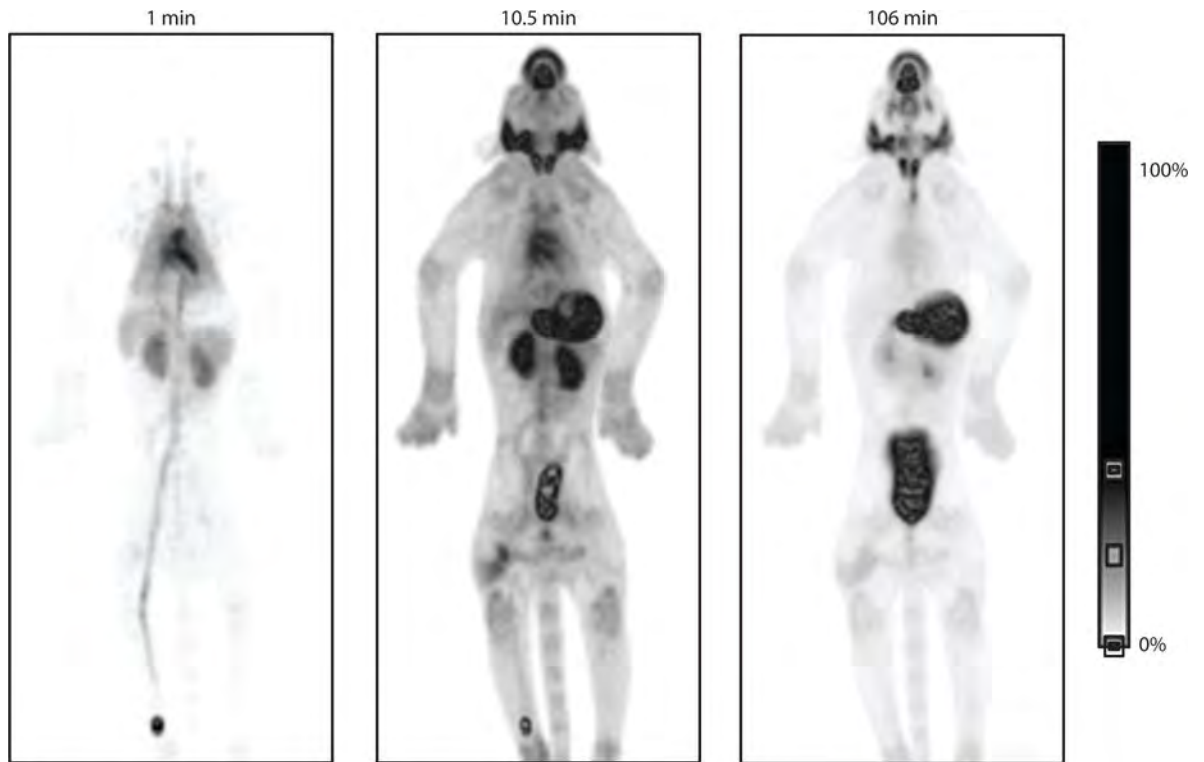
Figure 3.
Na$^+$/I$^-$ symporter (NIS)-mediated [^{18}F]-tetrafluoroborate biodistribution in macaques. Maximum-intensity projection positron emission tomography images of [^{18}F]-tetrafluoroborate at different time points following intravenous injection of the isotope. Adapted from Reference 54 under the terms of the Creative Commons Attribution 4.0 International License, http://creativecommons.org/licenses/by/4.0.
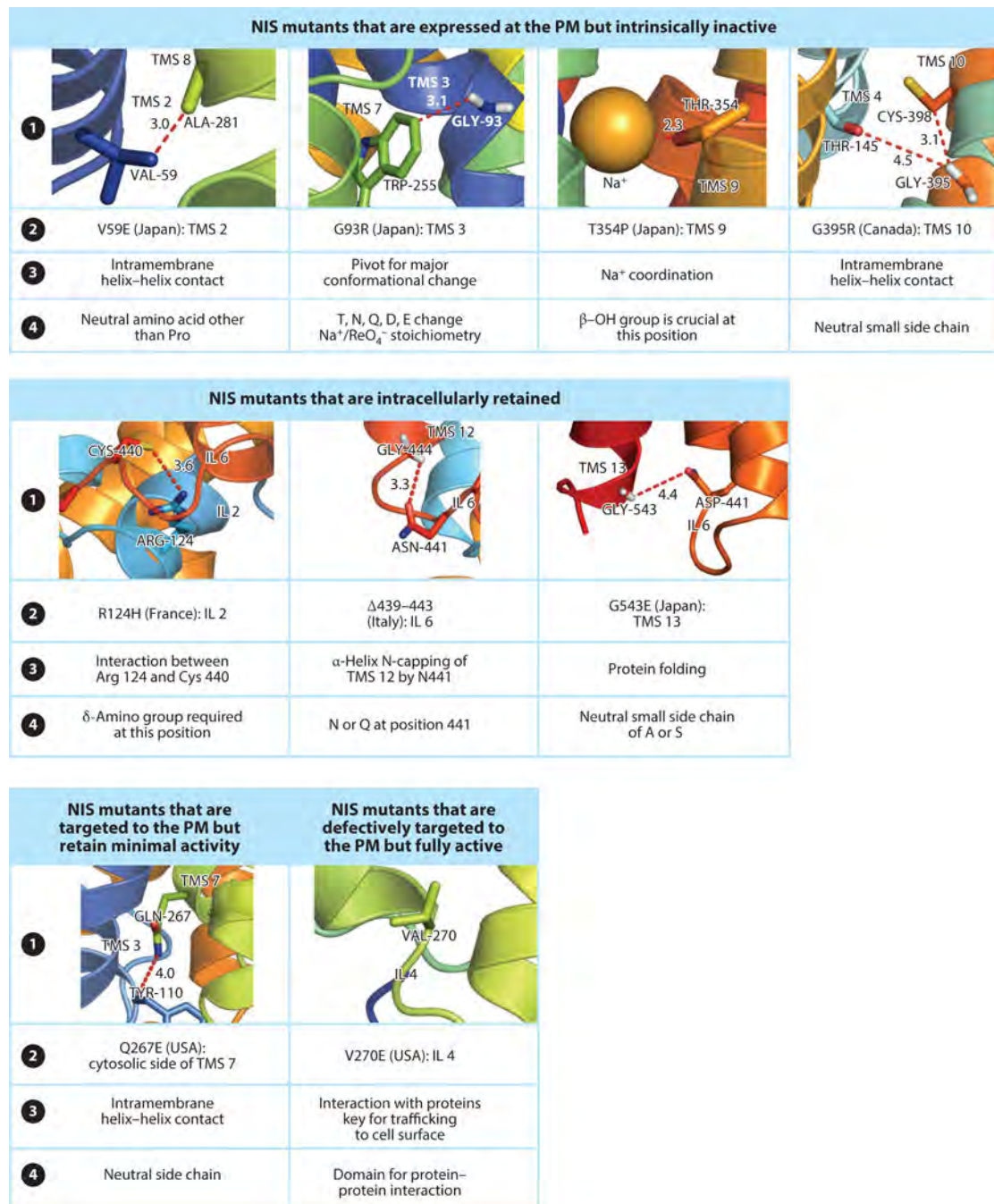
Figure 4.
Summary of properties of ITD-causing NIS mutations characterized at the molecular level. ❶ Residue interaction in the three-dimensional NIS homology model; ❷ amino acid substitution or deletion, country of origin of ITD patient, and mutation location in NIS; ❸ amino acid function at the relevant position; and ❹ molecular requirement at the position. Abbreviations: ITD, I⁻ transport defect; NIS, Na⁺/I⁻ symporter; PM, plasma membrane; TMS, transmembrane segment.

```
                 59              93              124            267            270
      NIS  ·· 57 LPVGL ··········· 91 CLGQL ············· 122 EMRFS ··········· 265 QVQRY ············· 268 RYVAC ····
    SMCT1  ·· 55 VPVAL ··········· 89 AFTYF ············· 120 ELRFN ··········· 263 QVQRY ············· 266 RYISC ····
    SMCT2  ·· 51 GPVGL ··········· 85 FIAYL ············· 116 QLRFN ··········· 259 TIQRC ············· 262 RCISC ····
     SMVT  ·· 69 LPVAL ··········· 103 GCCYF ············ 134 ELRFN ··········· 277 QVQRY ············· 280 RYLSS ····
    SGLT1  ·· 68 WPIGA ··········· 102 EWNAL ············ 133 RKRFG ··········· 297 IVQRC ············· 300 RCLSA ····
    SGLT2  ·· 65 WPVGA ··········· 99 EWNAL ············· 130 RKRFG ··········· 297 IVQRC ············· 300 RCLAG ····
    SGLT3  ·· 68 WPMGA ··········· 102 EWTSS ············ 133 KKRFG ··········· 297 IVQRC ············· 300 RCLCG ····
     SMIT  ·· 49 VAIGA ··········· 83 EFNAL ············· 114 SKRFG ··········· 282 IVQRV ············· 285 RVLAA ····
   SLC5A9  ·· 77 WPIGA ··········· 111 EWNMR ············ 163 KKRFG ··········· 322 IVQRS ············· 325 RSLSA ····
  SLC5A10  ·· 60 WPIGA ··········· 94 EWNAT ············· 125 QKRYG ··········· 284 IVQRS ············· 287 RSLSA ····
    vSGLT  ·· 54 WAVGA ··········· 88 EWMAA ············· 119 EQRFN ··········· 270 IIQRT ············· 263 RTLAA ····
     PutP  ·· 45 FVTAL ··········· 79 AIGLT ············· 115 TGRFE ··········· 254 ILARF ············· 257 RFMAA ····


                 354             395             441            543
      NIS  ··352 LSTAS··········· 393 IYGSA············· 439 ACNTP··············· 541 LCGAL·····
    SMCT1  ··350 LSTVS··········· 391 VYGAL············· 436 FANSI··············· 534 LVGIL·····
    SMCT2  ··346 LSTVA··········· 387 LFGVM············· 432 FVNWK··············· 517 VAGVI·····
     SMVT  ··364 LSTIS··········· 405 GYGLL············· 450 CANPP··············· 540 VVGLI·····
    SGLT1  ··391 MSSLT··········· 432 VLIGI············· 479 RVNEP··············· 539 ITIVV·····
    SGLT2  ··391 MSSLA··········· 432 FIVVV············· 479 RVNEQ··············· 539 LLTLT·····
    SGLT3  ··391 MSSLT··········· 432 LLTVV············· 479 RVNEQ··············· 539 LVTLG·····
     SMIT  ··376 MSDLD··········· 417 FMVVI············· 464 RCNEQ··············· 524 LITVI·····
   SLC5A9  ··416 MSSLT··········· 457 FLVVI············· 504 RVTEP··············· 564 IVIVI·····
  SLC5A10  ··394 MSSLT··········· 435 ALIGV············· 482 RANEQ··············· 542 AVVVA·····
    vSGLT  ··363 VSSLA··········· 405 VALVV············· 450 KTTSK··············· 496 FTSLS·····
     PutP  ··339 MSTLS··········· 381 VVALV············· 427 RN——··········································
```

Figure 5.
SLC5 family alignment. Residues corresponding to the NIS positions found mutated in ITD patients that have been characterized at the molecular level are highlighted in red. Rectangles represent NIS TMSs (colors are the same as in Figure 1*a*); lines represent intracellular loops in NIS. Abbreviations: ITD, I⁻ transport defect; NIS, Na⁺/I⁻ symporter; TMS, transmembrane segment.
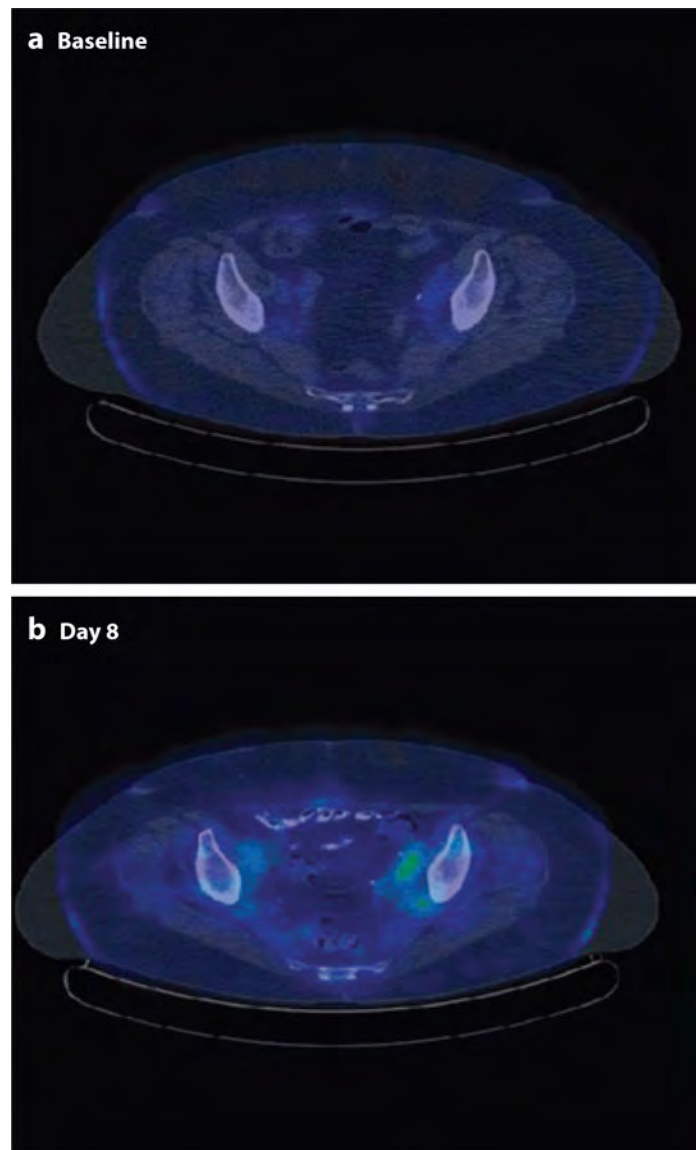
Figure 6.

NIS expression as imaged by $^{123}I^-$ uptake in one of the study patients. The $^{123}I^-$ SPECT/CT scan was negative at baseline (*a*) but became positive on day 8 of cycle 1 (*b*). Reprinted with permission from Reference 140. Copyright 2015, American Association for Cancer Research. Abbreviations: CT, computed tomography; NIS, Na$^+$/I$^-$ symporter; SPECT, single-photon emission computed tomography.

Table 1

Properties of various Na^+/I^- symporter (NIS) substrates

NIS substrate	Radioisotope	Covalent incorporation into TG	Stoichiometry	Decay/emission	Energy emission (MeV)	Decay time	Imaging technique
I^-	^{123}I	Yes	$2Na^+{:}1I^-$	EC/γ	0.159	13 h	SPECT
	^{125}I			EC/γ	0.027	59.4 days	
	^{131}I			β^-/γ	0.364	8 days	
	^{124}I			β^+	0.51	4.2 days	PET
TcO_4^-	^{99m}Tc	No	ND	IT/γ	0.14	6 h	SPECT
ReO_4^-	^{188}Re		$1Na^+{:}1ReO_4^-$	β^-/γ	0.155	17 h	
BF_4^-	^{18}F		ND	β^+	0.51	109 min	PET

Abbreviations: β^-, beta decay; β^+, positron decay; EC, electron capture; γ, gamma emission (high-energy photons); IT, isomeric transition; ND, no data; PET, positron emission tomography; SPECT, single-photon emission computed tomography; TG, thyroglobulin.